River flooding reshapes sediments, contaminants and benthic microbial communities in a Mediterranean coastal system

Claudio Pellegrini[1], Marco Basili[2], Irene Sammartino[1]*, Tommaso Tesi[3], Emanuela Frapiccini[2], Grazia Marina Quero[2-4], Sarah Pizzini[2-5-6], Roberta Zangrando[3-6], Gian Marco Luna[2-4], Sara Catena[1], Bruno Campo[7], Naomi Massaccesi[2-4-7], Fabio Trincardi[1], Andrea Gallerani[1], Jacopo Chiggiato[1]

[1] *National Research Council (CNR), Institute of Marine Science (ISMAR), Bologna, Italy*
[2] *National Research Council (CNR), Institute for Biological Resources and Marine Biotechnology (IRBIM), Ancona, Italy*
[3] *National Research Council (CNR), Institute of Polar Sciences (ISP), Bologna, Italy*
[4] *National Biodiversity Future Center (NBFC), Palermo, Italy*
[5] *Fano Marine Center (FMC), Fano, Italy*
[6] *Department of Environmental Sciences, Informatics and Statistics, Ca' Foscari University of Venice, Venezia, Italy*
[7] *Department of Biological, Geological and Environmental Sciences (BIGEA), University of Bologna (UNIBO), Bologna, Italy*

* *Correspondence to*: Irene Sammartino (irene.sammartino@cnr.it)

Abstract. This study examines the sedimentary and microbial responses offshore the Marche Region (Italy) to the September 2022 flood, one of the most severe recent hydrological events, which delivered large amounts of sediment and anthropogenic contaminants to the Adriatic Sea. We employed a multidisciplinary approach integrating sedimentology, geochemistry, organic matter analysis, pollutant assessments (Polycyclic Aromatic Hydrocarbons, PAHs and Poly- and Perfluorinated alkyl substances, PFASs), and benthic microbial community structure. Sediments collected just five days after the event offshore river mouths reveal that flood deposits, ranging from fine sand to coarse silt, remained substantially confined to the nearshore zone, whereas finer clay particles were dispersed further offshore and down to the 15 m isobath. This distribution reflects intense riverine inputs and a brief windstorm-enhanced coastal circulation that generated patchy, temporary sediment accumulations mainly in the prodelta sector. Simultaneously, the flood forced a strong spatial heterogeneity in benthic bacterial communities, through the introduction of short-distance shifts in sediment texture and organic matter content. Freshwater taxa became prominent in prodelta deposits, highlighting riverine sedimentary imprints. Heavy metal concentrations remained below regulatory thresholds, whereas organic pollutants, heterogeneously distributed, reach peak concentrations offshore urban and industrial zones. PAH signatures indicate mixed pyrogenic and petrogenic sources, while next-generation PFASs (6:2 FTS) showed localized but severe contamination linked to upstream industrial activities. Despite the flood's magnitude onshore, its offshore sedimentary signatures resulted ephemeral and spatially limited. These findings underscore the ecological significance of episodic sediment and contaminant input, while highlighting the challenges in detecting such transient events in the marine stratigraphic record.

1. INTRODUCTION

Climate warming is intensifying precipitation extremes globally, with record-breaking daily rainfall events increasing since the 1980s (Allan and Soden, 2008; Westra et al., 2013; Lehmann et al., 2015; Nie et al., 2018; Fowler et al., 2021; Merz et al., 2021; Sun et al., 2021; IPCC, 2023). These changes drive shifts in river discharge patterns and exacerbate flood hazards worldwide, which are expected to worsen due to urbanization, soil degradation, and expanding flood-prone areas (Kundzewicz et al., 2014; Blöschl et al., 2017; Semenza et al., 2020; Slater et al., 2021; Syvitski et al., 2022; Dottori et al., 2023). Extreme river floods abruptly alter coastal ecosystems by delivering freshwater (Vörösmarty et al., 2003), sediments (Rozemeijer et al., 2021; Xin et al., 2023), nutrients (Gao et al., 2018; Lin et al., 2022), organic matter (Bao et al., 2016; Bianchi et al., 2018), pollutants (Weiss et al., 2025; Adeoba et al., 2025), and microbes (Chen et al., 2018), that reshape salinity, sediment composition, and biogeochemical conditions (Gibson et al., 2002; Death et al., 2015; Lin et al., 2022; Ennas et al., 2024; Guid et al., 2024; Yao et al., 2024). River floods promote microbial dispersal and community shifts, impacting carbon cycling, redox processes, and contaminant dynamics (Reed and Martiny, 2013; Jia et al., 2017; Nakatsu et al., 2019; Wang et al., 2019; DesRosiers et al., 2022; Gao and Guo, 2022; Lin et al., 2022; Zhang et al., 2022, 2023; Li et al., 2024; Ning et al., 2024; Yao et al., 2024). However, how sedimentological controls such as grain-size-dependent transport modulate these biological responses during floods is still not well constrained.

In this scenario, small- to moderate-sized rivers (10^2–10^5 km^2 catchment extent), which are far more numerous than large rivers discharging into coastal zones, play a key role in sediment dynamics on continental shelves (Milliman and Meade, 1983; Syvitski and Kettner, 2007; Pitarch et al., 2019). Flood events in these rivers typically coincide with stormy marine conditions, influencing the preservation and spatial distribution of flood deposits offshore (Wheatcroft et al., 2006; Syvitski and Kettner, 2007; Pellegrini et al., 2021, 2024). Suspended sediment concentrations in such rivers increase non-linearly with discharge, making short-lived flood events the dominant mechanism of sediment delivery to coastal systems (Milliman and Syvitski, 1992; Syvitski et al., 2003; Cohen et al., 2022; Pierdomenico et al., 2022). In fact, most of the sediment flux from small rivers likely occurs during short-lived (days to weeks) flood events (e.g., Blöschl, 2000; Wheatcroft and Drake, 2003; Winsemius et al., 2016; Merz et al., 2021), highlighting the critical role of river floods in coastal sedimentation. Studying these river flood

deposits requires rapid event-response sampling, often challenging due to unpredictability and logistic constraints, especially in dynamic shallow-water environments like deltas where pollutant and microbial community distributions are critical but hard to access immediately post-flood (Wheatcroft, 2000; Trincardi et al., 2020; Pellegrini et al., 2023).

In recent decades, significant efforts have been made to understand the key depositional processes shaping subaqueous coastal environments (e.g., Kuehl et al., 1986; Goodbred et al., 2003; Bentley et al., 2006; Liu et al., 2006; Macquaker et al., 2010; Korus and Fielding, 2015; Hanebuth et al., 2021; Pellegrini et al., 2021; Lin et al., 2024; Vona et al., 2025). Sedimentary structures formed during floods reflect complex interactions of sediment supply, hydrodynamics, and biological processes, providing essential insights into depositional conditions and coastal sediment dynamics (Nittrouer et al., 1986; Bentley and Nittrouer, 2003; Bhattacharya and MacEachern, 2009; Jaramillo et al., 2009; Macquaker et al., 2010; Ainsworth et al., 2011; Peng et al., 2022; Pellegrini et al., 2024). Marine sediments also act as reactive interfaces and sink for contaminants, influencing marine food webs through episodic resuspension and bioaccumulation (Roberts, 2012). Benthic microbial communities at the sediment-water interface mediate organic matter degradation, nutrient cycling, and contaminant transformation, yet their spatial organization and responses to flood-driven sediment heterogeneity remain poorly understood (Danovaro et al., 2012; Voynova et al., 2017; Trouche et al., 2021).

Acting as both reactive interfaces and long-term sinks, coastal environments accumulate contaminants that can be episodically resuspended and bioaccumulated, with cascading effects across marine food webs (Roberts, 2012). Within this dynamic environment, benthic microbial communities occupy the critical boundary between the water column and the subseafloor (Voynova et al., 2017; Liu et al., 2020; Trouche et al., 2021), where they play fundamental roles in organic matter degradation, nutrient cycling, and contaminant transformation (Danovaro et al., 2012; Steichen et al., 2020; Checchi et al., 2021; Jiajun et al., 2024). Furthermore, hypopycnal coastal plumes foster intense new primary productivity, adding another source of organic biomass accumulating at the seafloor of the continental shelf (Lohrenz et al., 1990; Campanelli et al., 2011; Vona et al., 2025). Despite their importance, the factors controlling the spatial organization and functioning of these communities remain incompletely understood, particularly in dynamic coastal settings where sediment resuspension, alongshore transport, and temporary deposition interact with pronounced small-scale heterogeneity (Clark et al., 2021; Trouche et al., 2021).

Coastal systems are a temporary storage for river-borne sediments (e.g., Blair and Aller, 2012; Bao et al., 2016; Bianchi et al., 2018; Pellegrini et al., 2021, 2024) and can accumulate anthropogenic materials from catchments (Simon-Sánchez et al., 2019; Lim et al., 2021; Pierdomenico et al., 2022; Cecchetto et al., 2023; Pellegrini et al., 2023; Saliu et al., 2023; Trincardi et al., 2023; Bolan et al., 2024; Weiss et al., 2025; Bue et al., 2025; Gruca-Rokosz et al., 2025; Jalaosho et al., 2025; Nikki et al., 2025; Owowenu et al., 2025; Mancuso et al., 2026), especially in prodeltas, that are the delta sector lying beyond its front in a submerged environment where the highest sediment accumulation rates are reached (Coleman and Wright, 1975; Pellegrini et al., 2020). Riverine sediments play a fundamental role in the supply of hazardous metals and other contaminants to coastal areas, often reflecting significant sources of pollution (e.g., Lucchini et al., 2001; Sammartino, 2004; Amorosi and Sammartino, 2007; Jeon et al., 2011; Munoz et al., 2017; Amorosi et al., 2022; Riminucci et al., 2022; Frapiccini et al., 2024; Fanelli et al., 2025). Among coastal environments, river deltas respond rapidly to both natural and anthropogenic changes (Syvitski et al., 2005, 2009; Blum and Roberts, 2009; Overeem and Brakenridge, 2009; Falcini et al., 2012; Anthony et al., 2014; Bosman et al., 2020; Trincardi et al., 2020; Syvitski et al., 2022; Gardner et al., 2023; Haq and Milliman, 2023; Anthony et al., 2024; Warrick et al., 2024; Ohenhen et al., 2026).

This study addresses the highlighted gaps by studying the offshore impact of an exceptional river flood occurred in September 2022 in the Marche Region (Fig. 1). Samples were strategically collected from freshly deposited surface sediments and from underlying, pre-flood bottom deposits, allowing for a direct comparison to identify the effects of the flood. By capturing sedimentary, geochemical, and biological signals shortly after the event, we provide novel insights into early deposition processes and spatial patterns triggered by floods. The overall goal is to define the impact of major storm peaks, dramatically affecting small, steep, and sediment-laden ('dirty') river catchments, on coastal and offshore regions. Enhancing our ability to recognize the offshore consequences of these floods will improve the evaluation of pollutant dispersal and potential bioaccumulation originating from heavily anthropogenically impacted land areas.

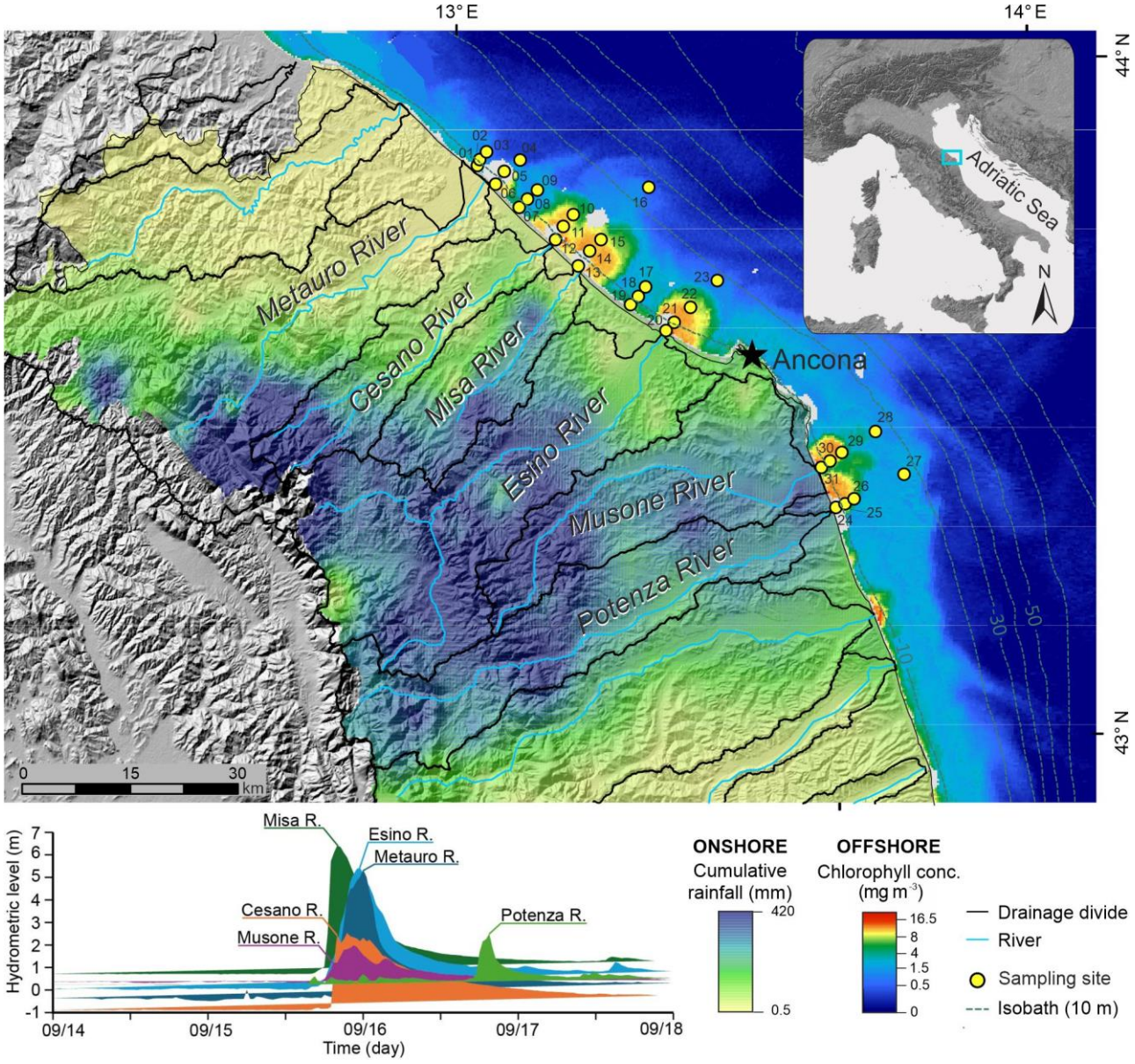

105

Figure 1: Study area showing cumulative rainfall (mm) recorded between September 15th and 16th, along with the catchments of major rivers affected by the September 2022 flood. Hydrometric levels along the rivers highlight abrupt variations occurring within a few hours. Yellow dots indicate sampling sites at sea. Offshore background shading represents satellite-derived chlorophyll-a concentration (mg m⁻³) on September 16th, used as a proxy for surface

110 **productivity (from EU Copernicus Marine Service product OCEANCOLOUR_MED_BGC_L3_MY_009_143).**

2. APPROACH

2.1 Study area and the 2022 flood event

On September 17th, a low-pressure system established over the central Adriatic Sea led to scattered, thought very intense, showers. While hydrodynamics conditions during the flood were still calm, this low-pressure system rapidly moved across the Adriatic Sea resulting (along the coast of the Marche Region) in gale-force northeasterlies during the afternoon (Figs. 2a, 2b, 2c), with rapid intensification of the sea state (Fig. 2d), and alongshore currents (ca. 120°; i.e. toward South-East, see Fig. 2f), with peaks during the windstorm of 1 m s^{-1} at the surface and 0.7 m s^{-1} near bottom (Fig. 2e). Operational ocean model data (Figs. 2g, 2h, 2i) provide a larger picture of the hydrodynamical response to the windstorm. Although this windstorm was short-lived, associated resuspension and transport alongshore arguably played a role in the fate of the sediment discharged by the flood to the coastal area, as discussed in Section 5.

The September 2022 rainfall event occurred after a prolonged period of drought, strongly impacting the catchment for approximately twelve hours (Donnini et al., 2023; Pulvirenti et al., 2023). On September 15th, several thunderstorms affected the northern and central mountainous and high-hilly areas of the region, with rainfall decreasing intensity while moving towards the coast. In the late afternoon, a self-regenerating and stationary system formed, eventually affecting the hills and coastal areas. This system led to critical conditions particularly in the Cesano and Misa rivers basins (De Lucia et al., 2024), with cumulated rain values peaking up to 90 mm / 1 h and 400 mm / 6 h (data from the Marche Region, Regional Functional Center). Consequently, river levels rose rapidly, by up to five meters in just three hours (Fig. 1), with flood thresholds exceeding multiple sites and widespread inundations reported. On the following day, a similar, yet weaker, thunderstorm system developed to the windward side of the Apennines, affecting additional catchments to the South (i.e. Potenza River, see Fig. 1), with cumulated rain peaking up to 140 mm over the event.

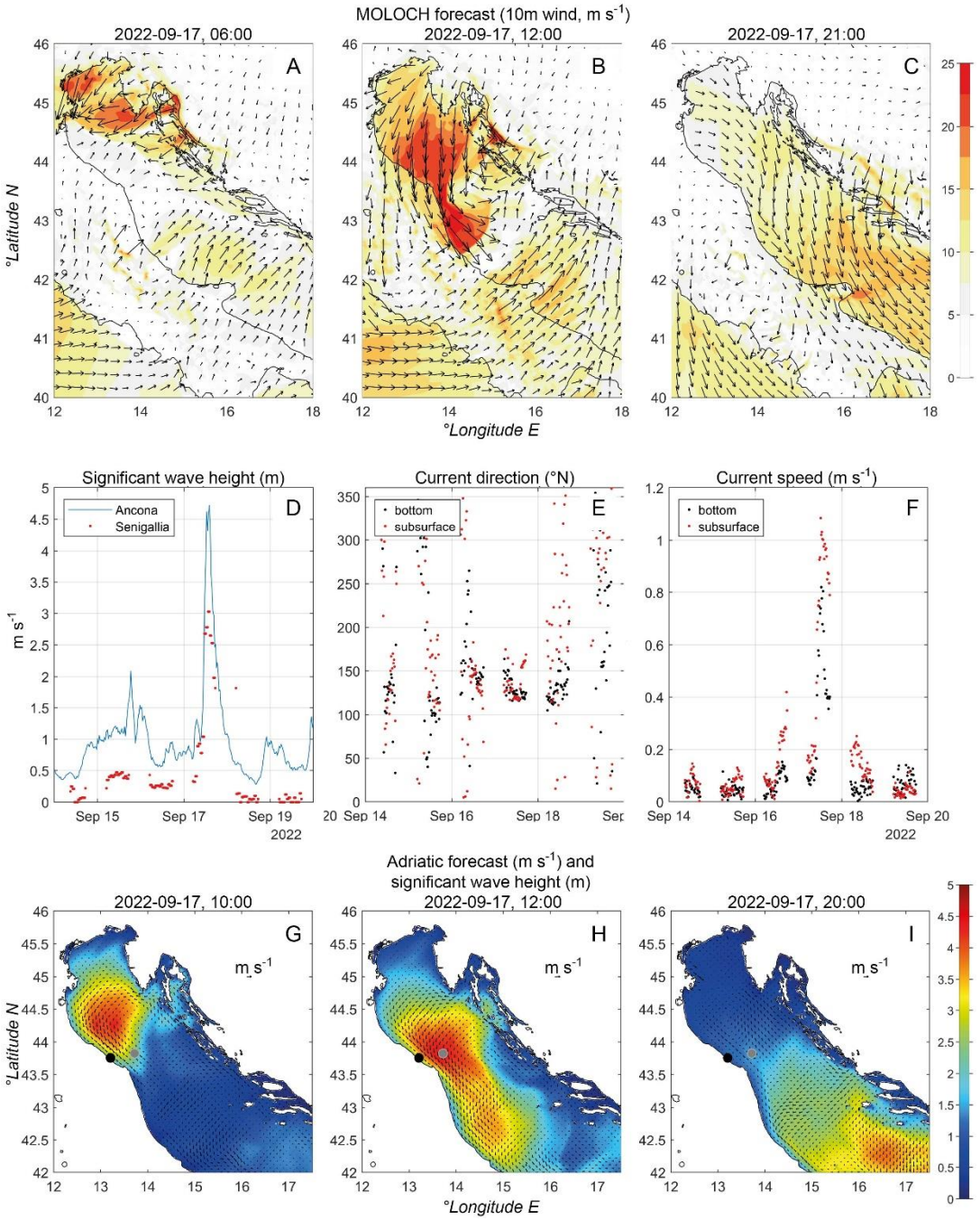

135 **Figure 2: 10 m wind (m s^{-1}) MOLOCH model forecast valid time September 17th, 2022 (A) 06:00 UTC, (B) 12:00 UTC, (C) 21:00 UTC; significant wave height (m) measured at Ancona (blue line) wave buoy and Senigallia (red dots) marine weather station (D), ocean currents speed (m s^{-1}) measured by TeleSenigallia Acoustic Doppler Current Profiler, ADCP**

(E), along with (F) currents' direction (degree, 0° N, flowing toward); Adriac model forecast for significant wave height (m, color coded) and surface currents (black arrows) valid time September 17th, 2022 (G) 10:00 UTC, (H) 13:00 UTC, (I) 20:00 UTC. The black filled circle indicates TeleSenigallia marine weather station position. The gray filled circle indicates the Aancona wave buoy position. Technical details on the source datasets can be found in the Supplement.

2.2 The 2022 Rapid Response Cruise (RRC)

Sediment samples were collected on board the R/V *Tecnopesca II* on September 23rd, 2022, just five days after the major flooding event that impacted the central Adriatic coast. Sampling took place along nine coast-to-offshore transects, corresponding to the six primary river mouths affected by the flood, as well as three intermediate transects (Fig. 1). The number of sampling stations extended offshore until flood-related deposits were no longer detectable. The flood event produced a distinctive sedimentary deposit, identifiable by its fabric characteristics (i.e. grain size and shape, color, organic matter and water content, sedimentary structures; Lazar et al., 2015), relative to the underlying sediments. Sediment was retrieved from each station using a 25 L Van Veen grab, which allowed the recovery of approximately 60 kg (25,000 cm^3 x 2.5 g cm^{-3}) of sediment. The grab allowed for the sub-sampling of the sediment succession up to 25 cm in depth to examine the sedimentary expression of the 2022 flood event (Fig. 3).

For each sampling point, two aliquots of sediment were taken: the first one (top) corresponding to the 2022 river flood deposits, the second one (bottom) corresponding to pre-flood sedimentary deposits. All sub-samples were labelled with the cruise acronym (Rapid Response Cruise, RRC) and stored in decontaminated or sterilized glass vials. Organic pollutant analyses were carried out on a subset of sediment samples. Specifically, two sampling points for each of the nine analyzed transects were selected: the first one is located closer to the coast, the second one at the furthest point. All the analyses are summarized in Table S1 in the Supplement.

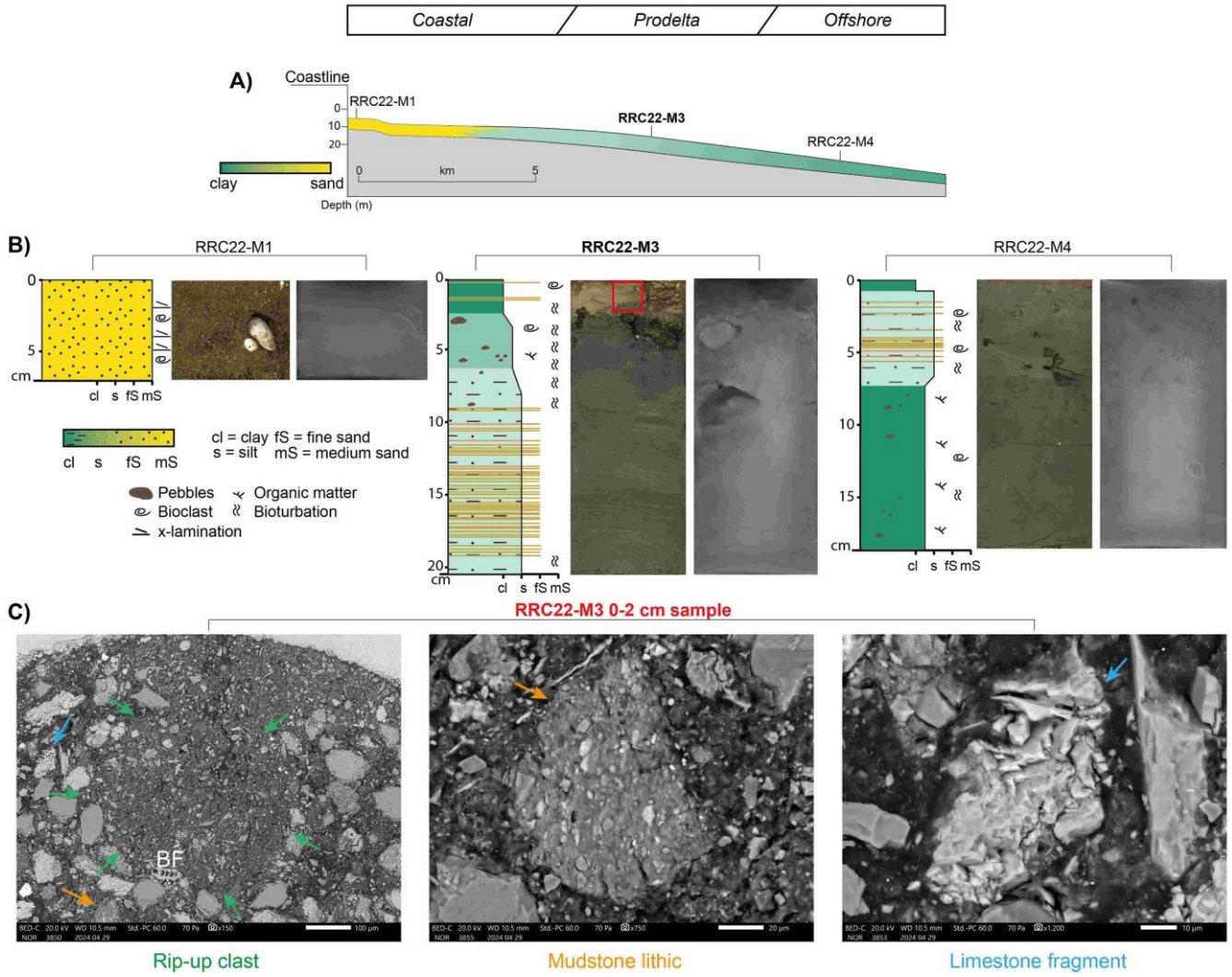

160

Figure 3: The sedimentary expression of the 2022 river flood along a coast-to-sea transect offshore from the Misa River: A) schematic section based on previously published seismic profiles (e.g., Cattaneo et al., 2003; Pellegrini et al., 2021); B) sedimentary logs illustrating the main lithological changes, sedimentary structures, bioclasts, and bioturbation features. Red square on sediment core RRC22-M3 marks the sampling position of the 2022 river-flood sediments (0-2

165 **cm) analyzed by Scanning Electron Microscope (SEM); C) SEM images of a representative river-flood sediment sample**

(RRC-M3, 0-2 cm) from the offshore Misa transect, showing fine-grained intraclasts, semi-consolidated rip-up clast (green arrows), mudstone lithic (orange arrows), limestone fragment (light blue arrows), benthic foraminifera (BF).

3. DATA AND METHODS

3.1 Sedimentological analyses on inorganic and organic particles

Sedimentological analyses were conducted at multiple scales, from meter to micron-nanometer resolution. Stratigraphic descriptions coupled with high-resolution photographic images allowed characterization of subtle sedimentary structures in fine-grained sediments (Fig. 3a, b). Samples with notable texture changes were selected for Scanning Electron Microscopy (SEM) to investigate sediment fabric and sedimentary processes (Fig. 3c). SEM analysis was performed on samples stabilized with resin after pore water removal and ion milling, following established protocols (Schieber, 2013; Schimmelmann et al., 2015; Pellegrini et al., 2021, 2024; see Supplement). SEM surfaces were examined in low vacuum mode without conductive coating, and Energy Dispersive X-ray Spectroscopy (EDS) was used for compositional analysis.

Granulometric analysis and water content determination were conducted on sediment aliquots from each station, for both flood and pre-flood deposits. Grain size was measured using a Malvern Panalytical Mastersizer 3000 analyzer (0.01–3500 µm), with samples dispersed and ultrasonicated prior to analysis. Grain-size distributions were processed and reported according to the Wentworth scale (Wentworth, 1922; Blott and Pye, 2001; see Supplement).

Organic matter was characterized at bulk and molecular levels. Samples were freeze-dried, homogenized, and approximately 15 mg was weighed into silver boats. The samples were acidified with 1.5 M HCl and dried at 55 °C. Analyses were conducted using a Thermo Fisher Scientific Delta Q IRMS coupled with a FLASH 2000 CHNS Analyzer via a CONFLO IV gas mixing system. Measurement of uncertainties was assessed based on replicate analyses of an in-house standard. Uncertainties were <3% for TOC and <4% for TN, expressed as coefficients of variation of the measured values. For $\delta^{13}C$, the analytical precision (1σ) was <0.1‰. All $\delta^{13}C$ values are reported in per mil (‰) relative to the V-PDB standard. A compilation of $\delta^{13}C$ data from terrigenous sources along the Adriatic coast was used to define endmembers for source apportionment (Tesi et al., 2013; Pellegrini et al., 2021, see Supplement).

3.2 X-Ray Fluorescence (XRF)

Geochemical analyses of bulk sediments were conducted using Wavelength Dispersive X-Ray Fluorescence (WD-XRF) to quantify major and trace elements. Forty-two sediment samples were air-dried, ground, and pressed into tablets for analysis at the University of Bologna. Matrix correction methods and accuracy verification via Certified Reference Materials (CRMs) ensured reliable quantification (Franzini et al., 1972, 1975; Leoni and Saitta, 1976; Leoni et al., 1982; Govindaraju, 1989; see Supplement). Sediment provenance was assessed by comparing geochemical fingerprints to riverine deposits from Alpine and Apennine catchments, which display characteristic elemental signatures reflecting their lithology (Dinelli and Lucchini, 1999; Amorosi et al., 2022). Provenance indicators such as Ca-Al_2O_3, Cr-V, and MgO-Ni/Al_2O_3 diagrams were used for interpretation based on background knowledge (Amorosi et al., 2022).

3.3 Polycyclic Aromatic Hydrocarbons (PAHs)

Total PAH concentrations were determined only in surface sediments from a subset of 18 samples. The sixteen priority Polycyclic Aromatic Hydrocarbons (PAHs) identified by the US Environmental Protection Agency (EPA) were quantified to assess contamination sources. An ultrasonic-assisted solvent extraction was performed, followed by Ultra High-Performance Liquid Chromatography (UHPLC) analysis with diode array and fluorescence detection (Frapiccini et al., 2024; see Supplement). Method validation complied with ICH Q2B guidelines of the European Medicines Agency, and recoveries were verified with International Atomic Energy Agency (IAEA) CRMs.

Diagnostic ratios (i.e. Low Molecular Weight (LMW) / High Molecular Weight (HMW) compounds, anthracene / (anthracene + phenanthrene), ΣCOMB (combustion-related compounds) / ΣPAHs, fluoranthene / (fluoranthene + pyrene), benz[*a*]anthracene / (benz[*a*]anthracene + chrysene)) were calculated to distinguish petrogenic from pyrogenic PAH sources, following literature standards (Yunker et al., 2002; Arienzo et al., 2017; Maletić et al., 2019; Lee et al., 2021; Mali et al., 2022). For more detail see Tables S1, S2 and S3 and Figure S1.

3.4 Poly- and Perfluorinated alkyl substances (PFASs)

Total concentrations of Poly- and Perfluorinated alkyl substances (PFASs; ng g^{-1} dw) in surface sediment samples, both offshore and coastal, are shown in Table S1 and Table S4 in the Supplement. PFASs were extracted from sediment samples using an Accelerated Solvent Extractor (ASE) and methanol as an extraction solvent. Extracts were purified by Solid Phase Extraction (SPE) and analyzed using HPLC coupled with a triple quadrupole tandem Mass Spectrometer (MS/MS), equipped with an ElectroSpray Ionization (ESI) source, operated in negative polarity. Seventeen PFASs, including target and next-generation compounds, were quantified using internal standards and the isotopic dilution technique. The analytical method quality control followed US EPA 1663A guidelines, with repeatability, trueness, and recovery tests conducted on Pleistocene sediment fortified blanks (Pizzini et al., 2024; see Supplement). Results were corrected using instrumental response factors and are reported on a dry weight (dw) basis.

3.5 Microbial communities

Surface sediment samples (i.e., 2022 flood event samples) were investigated (see also Supplement). DNA was extracted from the top 0–1 cm sediment layer and amplified targeting the V4–V5 region of the 16S rRNA gene (Parada et al., 2016). Libraries were prepared using the Nextera protocol and sequenced on the Illumina NextSeq 2000 platform (2 × 300 bp). Raw data were processed with Cutadapt for adapter removal, and DADA2 for quality filtering, chimera removal, and Amplicon Sequence Variant (ASV) inference (Callahan et al., 2016; Basili et al., 2021). Taxonomic classification was performed using SILVA v138, excluding chloroplast and eukaryotic sequences. Abundance normalization and diversity analyses were conducted in R using *vegan* and *phyloseq* packages (McMurdie and Holmes, 2013; Oksanen et al., 2025). Linear discriminant analysis effect size (LEfSe) was performed to identify taxa characterizing the coastal, prodelta, and offshore groups, and the results were visualized using the ggplot2 package (version 3.5.1). For more details readers are referred to Supplement (Tab. S1, and Figure S2 and S3).

4. RESULTS

4.1 Spatial distribution of inorganic and organic particles

Grain size analyses reveal a slight decreasing trend in particle size in the 2022 river flood deposit, distinctive from older deposits. Additionally, a progressive decrease in particle size is observed along all coast-normal transects (Fig. 4). Fine sand to coarse silt is primarily confined near the coastline and at less than 10 m water depth (Fig. 4), where sedimentary structures with oblique- and cross-lamination are present (Fig. 3b). In contrast, further offshore muddy beds show an irregular surface at base and an overall fining up deposit (Figs. 3b, 4). The flood deposit shows relatively high bioturbation, few rounded pebbles, clasts, and bioclasts content (Fig. 3b, c). SEM imaging shows slightly sorted mudstone matrix with semi-consolidated clasts, detrital carbonate debris, and muscovite flakes (Fig. 3c). Mudstone lithics can contain pyrite grains that likely were oxidized through outcrop weathering; limestone fragments are abundant (Fig. 3c). Metal distribution in the flood sediment, reported in boxplot diagrams, shows concentrations much lower than the Italian permissible limits (Fig. 5). The flood deposits thin progressively seaward and are not present beyond the 15 m isobath (Figs. 3b, 4). Total Organic Carbon (TOC) increases by up to one order of magnitude in seaward sectors, reaching up to 1.2% (Fig. 4). Concurrently, $\delta^{13}C$ data indicate relatively higher OC_{Terr} concentrations, especially seaward of the Misa and Esino rivers (Fig. 4). Notably, fine sand laminations are observed only in sediments deposited prior to the 2022 event (Fig. 3b). These earlier sediments exhibit lower TOC content and more depleted $\delta^{13}C$ values (Fig. 4). For all elements, pre-flood sediments record values slightly lower than the flood ones. Only two samples, 04 (Metauro3) and 05 (Metauro2) from the Metauro River transect, revealed two outliers (values exceeding 1.5 times the interquartile range) for Cu, with concentrations of 50 and 56 mg kg^{-1}, respectively, however well below the threshold limit of 120 mg kg^{-1} (Fig. 5).

As shown by the scatterplot diagrams (Fig. 6), sediment supplied from the Po River shows high Cr and Ni concentrations, whereas relatively high Ca content typifies the Apennine provenance. Consistent with their geographic location close to the fluvial mouths of Apennine rivers, almost all samples plot in the field of Apennine composition, with the sole exception of sample 16 (collected >15 km from the coast), which is characterized by lower Ca and higher Cr concentrations and likely reflects Po River influence via the longshore currents. In general, there is strong overlap in composition between flood and pre-flood samples (Fig. 5), suggesting continuous supply from the Apennine rivers, regardless of the competence of individual flood events (Fig. 6).

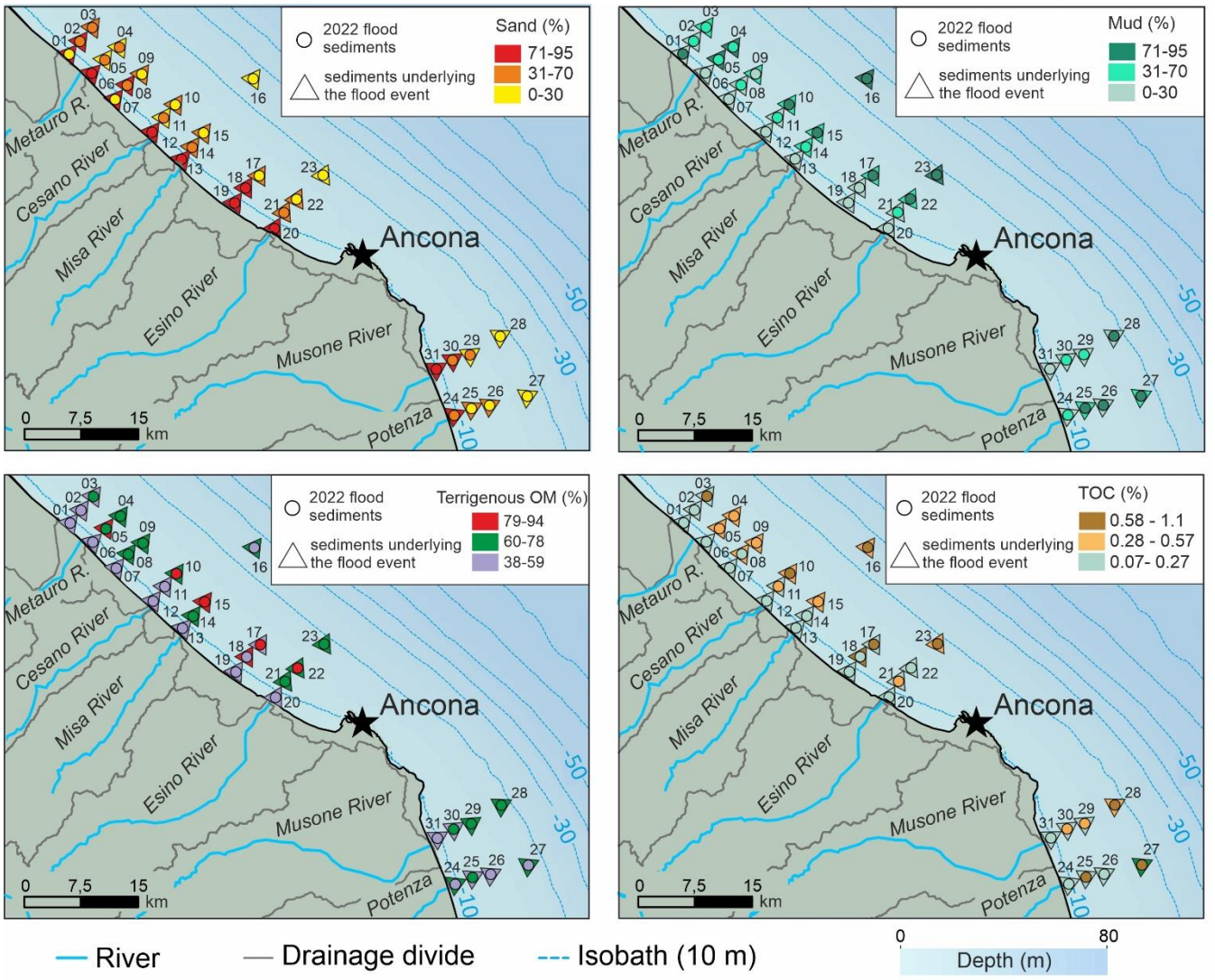

Figure 4: Sediment properties and geochemical parameters in the coastal, prodelta , and offshore areas of the Marche Region. Maps show distributions of sand (%), mud (%), terrigenous organic matter concentration (OM_{Terr}, %), and Total Organic Carbon (TOC, %) at sampling stations. Colored circles represent measured values for river flood sediments deposited in 2022, whereas colored triangles represent measured values in older underlying sediments. Background shading indicates bathymetric variations (dashed lines are 10 m isobaths); rivers and drainage divides are also shown.

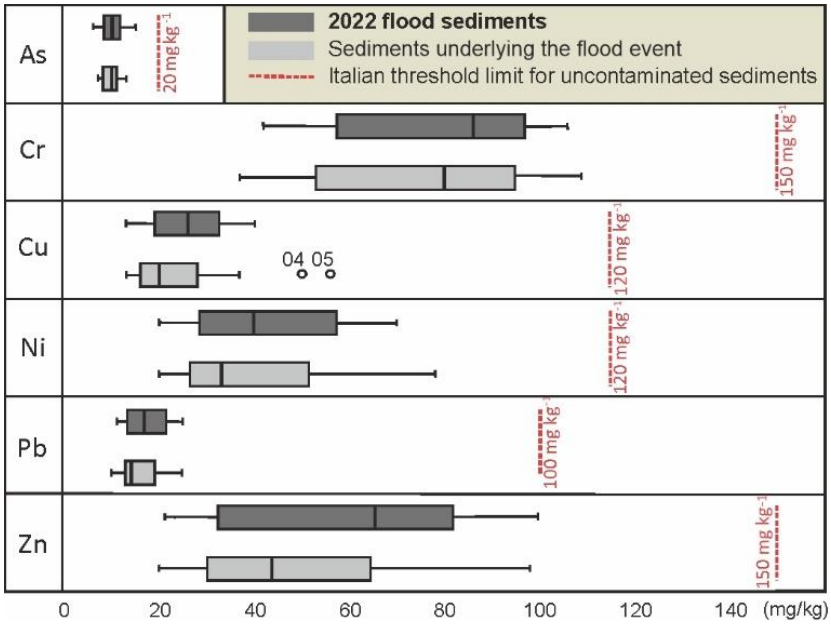

Figure 5: Boxplots of metal concentrations (mg kg^{-1}) in river flood sediments deposited in 2022 (dark gray boxes) and in older underlying sediments (light gray boxes) for As, Cr, Cu, Ni, Pb, and Zn. Dashed red lines indicate Italian sediment quality guideline thresholds. Outliers are shown as open circles.

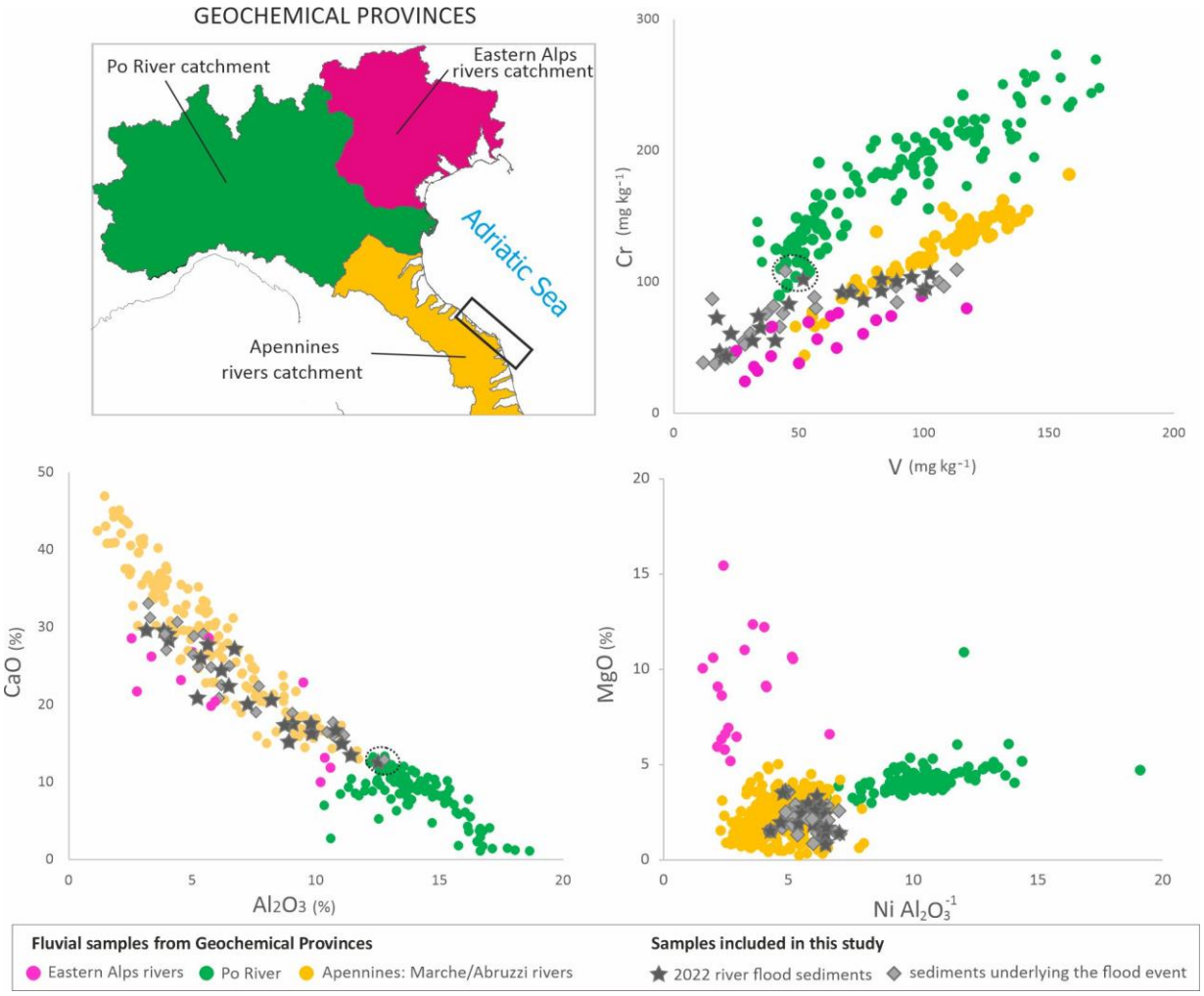

Figure 6: Main geochemical provinces of northern and central Adriatic Sea as documented in Amorosi et al., 2022, with the study area outlined (black box), along with scatterplot diagrams of selected geochemical indicators of sediment provenance. The geochemical composition of sediment from the Po River catchment has high Cr and Ni/Al_2O_3 and low CaO values. Sediments from the Eastern Alps catchment exhibit high CaO and MgO values, along with low Cr and Ni/Al_2O_3 values. Sediments from Marche/Abruzzi Apennines show high CaO and low Cr, Ni/Al_2O_3, and MgO values. Samples analyzed in this study (gray dots and diamonds) are consistent with an Apennine origin of the sediment from the Marche/Abruzzi catchments, except for samples from site 16 (black dashed line) which can be related to a mixed

Apennine-Po River provenance. Major and trace element data were used to evaluate sediment provenance through elemental ratio diagrams such as Ca-Al_2O_3, Cr-V, and MgO-Ni/Al_2O_3 (Dinelli and Lucchini, 1999; Amorosi et al., 2022).

285

4.2 Polycyclic Aromatic Hydrocarbons (PAHs)

Total PAH concentrations differed among the various sampling sites, with the highest values found at the site sampled offshore of the Misa River (15 - Misa3, 141 ng g^{-1} dw), the river most affected by the flood event in the Marche Region, and lower
290 values at the sampling site offshore of the Potenza River (26 - Potenza3, 15 ng g^{-1} dw), less impacted by the flood event. In general, a consistent trend is observed across the sampled transects, with higher values at offshore sites compared to coastal ones (Fig. 7). The most common PAHs at coastal sites are acenaphthylene and fluoranthene, while the most common PAHs at offshore sites are acenaphthylene and phenanthrene. In all sediment samples analyzed, HMW PAHs were below 5 ng g^{-1} dw (Fig. 7). Statistically significant differences (Mann-Whitman, $p > 0.05$) between coastal and offshore samples were recorded
295 for all individual PAHs, except for naphthalene, acenaphthene, fluorene, and fluoranthene. Notably, the Misa River transect showed the largest difference between the offshore site (15 - Misa3, 141 ng g^{-1} dw) and the coastal one (13 - Misa1, 25 ng g^{-1} dw). Higher values in the open sea compared to the coastal ones were also observed in the Cesano (69 vs. 27 ng g^{-1} dw) and Metauro (50 vs. 18 ng g^{-1} dw) river transects. A discrepancy in this pattern was observed in the Potenza River transect, where the values at the offshore site were lower than the coastal ones (15 vs. 43 ng g^{-1} dw). Some transects showed no significant
300 difference between offshore and coastal sites, such as the transects at station A (52 vs. 47 ng g^{-1} dw) and station C (30 vs. 31 ng g^{-1} dw).

Figure S1 shows the percentage contribution of each individual PAH to their total amount. In most of the marine sediment analyzed, LMW compounds dominate, accounting for over 50% of the total PAHs. An exception is the sediment sample collected near the mouth of the Potenza River (24 - Potenza1), where the predominant PAH is fluoranthene, a four-ring
305 aromatic compound considered HMW, which accounts for more than 40% of the total PAHs.

PAH isomer indicators, such as *anthracene / (anthracene + phenanthrene)*, *fluoranthene / (fluoranthene + pyrene)*, and *benz(a)anthracene / (benz(a)anthracene + chrysene*) ratios, show that the dominant sources for the investigated PAHs are

primarily combustion-related (Fig. 8). Samples close to the coastline, 24 - Potenza1 and, in smaller amount, 12 - Cesano1 and 19 - C1 sites, show a strong dominance of PAHs with pyrogenic sources. In all other cases, *LMW/HMW* and *ΣCOMB/ΣPAHs* ratios indicated a petrogenic source for the samples, particularly in the sediments collected North of the flood event, and far from the coast (01 - A1, 04 - Metauro3, and 09 - B3). Otherwise, 24 - Potenza1 site confirmed its pyrolytic origin. Finally, 03 - A3 and 29 - Musone3 sites are more closely related to a petrogenic origin than a pyrogenic one (Fig. 8).

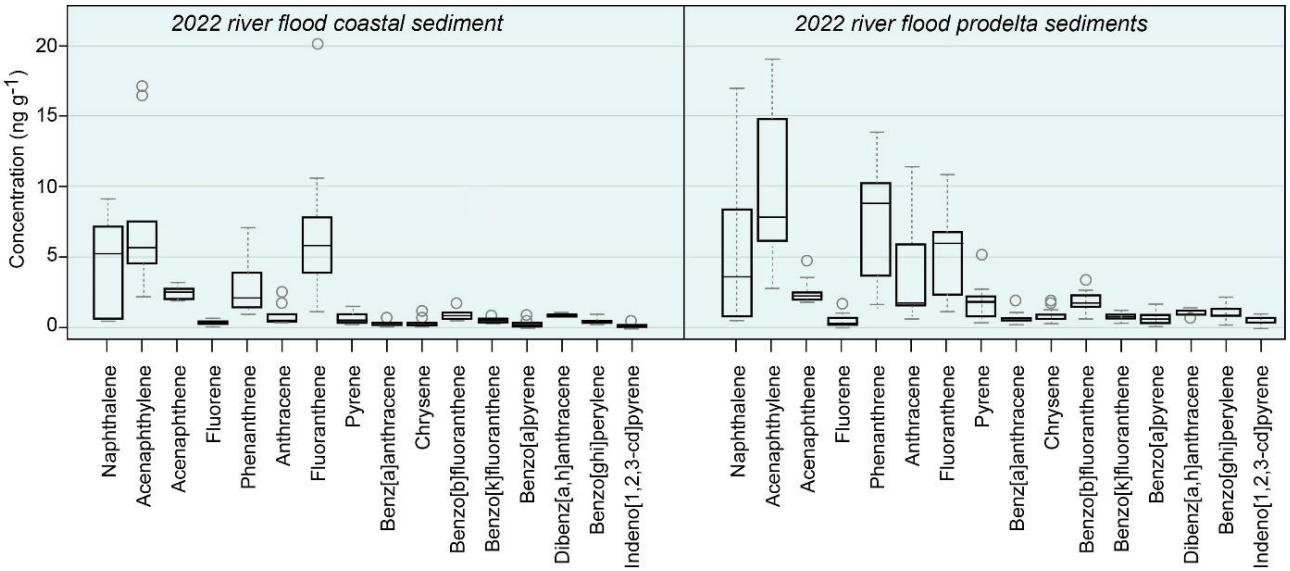

Figure 7: Boxplots of Polycyclic Aromatic Hydrocarbons concentrations (ng g^{-1} dry weight) in river flood sediments deposited in 2022, showing the distribution of individual compounds and highlighting differences in composition and levels between coastal and prodelta sectors. Outliers are shown as open circles.

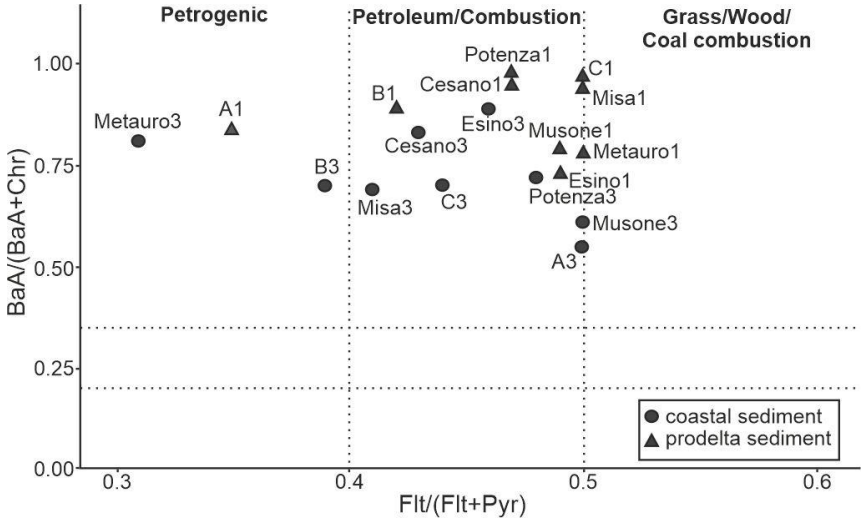

320 **Figure 8: Plot of the isomeric diagnostic ratios BaA/(BaA+Chr) vs. Flt/(Flt+Pyr) to infer the origin of Polycyclic Aromatic Hydrocarbons in river flood sediments deposited in 2022. Coastal sites (triangles) and prodelta sites (circles) are classified into petrogenic, petroleum/combustion, and biomass/coal combustion sources based on threshold values (dashed lines) from literature. BaA: benz(*a*)anthracene; Chr: chrysene; Flt: fluoranthene; Pyr: pyrene.**

325 4.*3 Poly- and Perfluorinated alkyl substances (PFASs)*

Among the seventeen investigated PFASs, only six compounds were detected in the sediment samples: four belonging to the traditional target group and two fluorotelomer classified as next-generation PFASs. All other PFASs were below the Method Quantification Limits (MQLs; Table S4). Furthermore, a large proportion of the samples corresponding to the deeper, pre-flood sediment layers showed no detectable PFAS contamination. Where contamination was observed, it was exclusively

330 attributable to 6:2 FTS (fluorotelomer sulfonate), detected in the range 0.127-0.355 ng g^{-1} dw, in scattered locations across the northernmost transects (A, Metauro River, B, Cesano River). Considering sediments deposited during the 2022 river flood, 6:2 FTS remained the predominant compound, followed by an 8:2 FTS contamination of lesser extent (Fig. 9). These sulfonated fluorotelomers are considered next-generation PFASs, commonly used as replacements for legacy compounds due to regulatory restrictions. Nevertheless, they are known for their high environmental persistence (Field and Seow, 2017). 6:2

335 FTS was detected at consistently higher concentrations than those in the corresponding pre-flood layers (approximately two

orders of magnitude greater), with values ranging from 0.203 to 86.10 ng g^{-1} dw. This compound was detected both offshore and nearshore, with a general decreasing trend observed along almost all coastal-to-offshore transects. 8:2 FTS was also detected in the surface sediments, though at lower concentrations (0.210-0.439 ng g^{-1} dw), and only in transects A (offshore, sample 03 - A3), Metauro River and B (both sampling points), and in the coastal sampling point of the Misa River transect (13 - Misa 1).

Perfluorohexanoic acid (PFHxA), perfluorooctanoic acid (PFOA), and perfluoroundecanoic acid (PFUnA) were each detected only in one sample, collected from the seaward sector of the Metauro River transect (04 - Metauro3), at concentrations of 0.120, 0.127, and 0.208 ng g^{-1} dw, respectively. Perfluorooctanesulfonic acid (PFOS), the only perfluorinated sulfonic acid (PFSA) identified, was detected exclusively in the seaward sector of the Esino River transect (22 - Esino3), at a concentration of 0.052 ng g^{-1} dw, suggesting a very limited distribution of this compound across the study area. No PFASs were detected in transects associated with the Musone and Potenza rivers, both located South of the Ancona Promontory (Fig. 9).

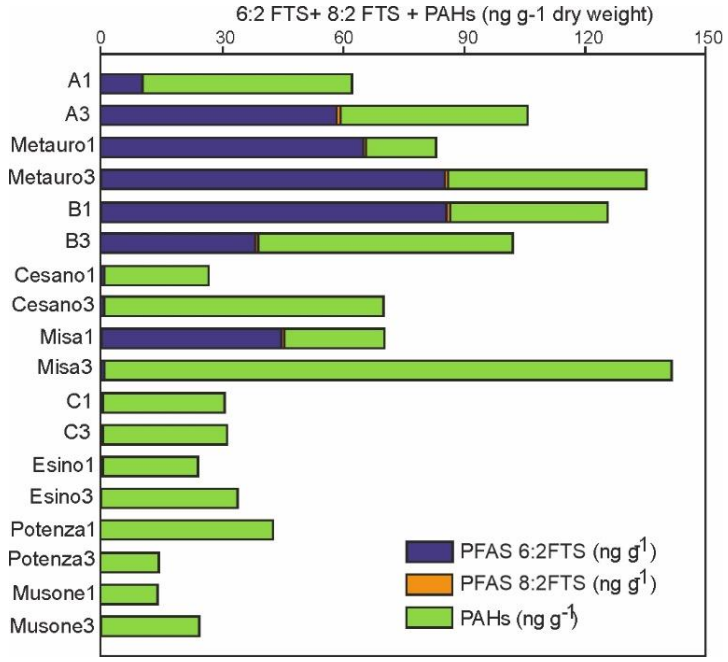

Figure 9: Stacked bar chart showing the relative abundance of the sulfonated fluorotelomers 6:2 FTS, 8:2 FTS (next-generation Poly- and Perfluorinated alkyl substances), and total Polycyclic Aromatic Hydrocarbons (PAHs) in river flood sediments deposited in 2022, across all sampling locations.

4.4 Microbial communities

Microbial diversity increased progressively with distance from shore. Statistical analyses revealed significantly lower Shannon diversity values in samples collected closer to the coast (ANOVA, $p < 0.01$), particularly compared to offshore samples (Tukey's test, $p < 0.01$). A similar, though not statistically significant, trend was observed for richness values (Fig. 10 a). Beta diversity analyses (Fig. 10b) revealed a clear spatial gradient in benthic prokaryotic community structure along the coast-to-offshore transects (ANOSIM, $p = 0.001$, $R = 0.6$), largely reflecting variations in sediment grain size, except for samples from the Musone River. Offshore samples formed a distinct cluster further composed of two subgroups, one associated with silt and one with clay, TOC and Total Nitrogen (TN; Fig. 10b). All samples were dominated by Gammaproteobacteria (average $26.39 \pm 2.61\%$), Bacteroidia ($10.14 \pm 3.35\%$), Thermoanaerobaculia ($7.49 \pm 2.42\%$), and Planctomycetes ($7.02 \pm 1.41\%$), with noticeable variability observed in their relative abundances from coastal to offshore sites (Fig. S2).

LEfSe (Linear discriminant analysis Effect Size) analysis (Fig. 10c) was conducted to identify microbial taxa significantly associated with sample groups defined by their distance from the coast and flood impact. Coastal samples were significantly ($p < 0.001$) enriched in Thermoanaerobaculaceae, Pirellulaceae, and Woeseiaceae (genus *Woesia*), whereas prodelta samples were characterized by the Desulfobulbaceae. Offshore samples displayed a higher relative abundance of Vicinamibacteria, Flavobacteriaceae, and Cyclobacteriaceae (Fig. 10c).

To further assess riverine influence, we screened all samples for the presence of freshwater-indicator taxa. Results showed that these taxa (i.e. *Flavobacterium*, *Variovorax*) were retrieved in offshore samples associated with clay, TOC, and TN (Fig. S3), whereas they were largely absent or rare in coastal and silt-associated offshore sites.

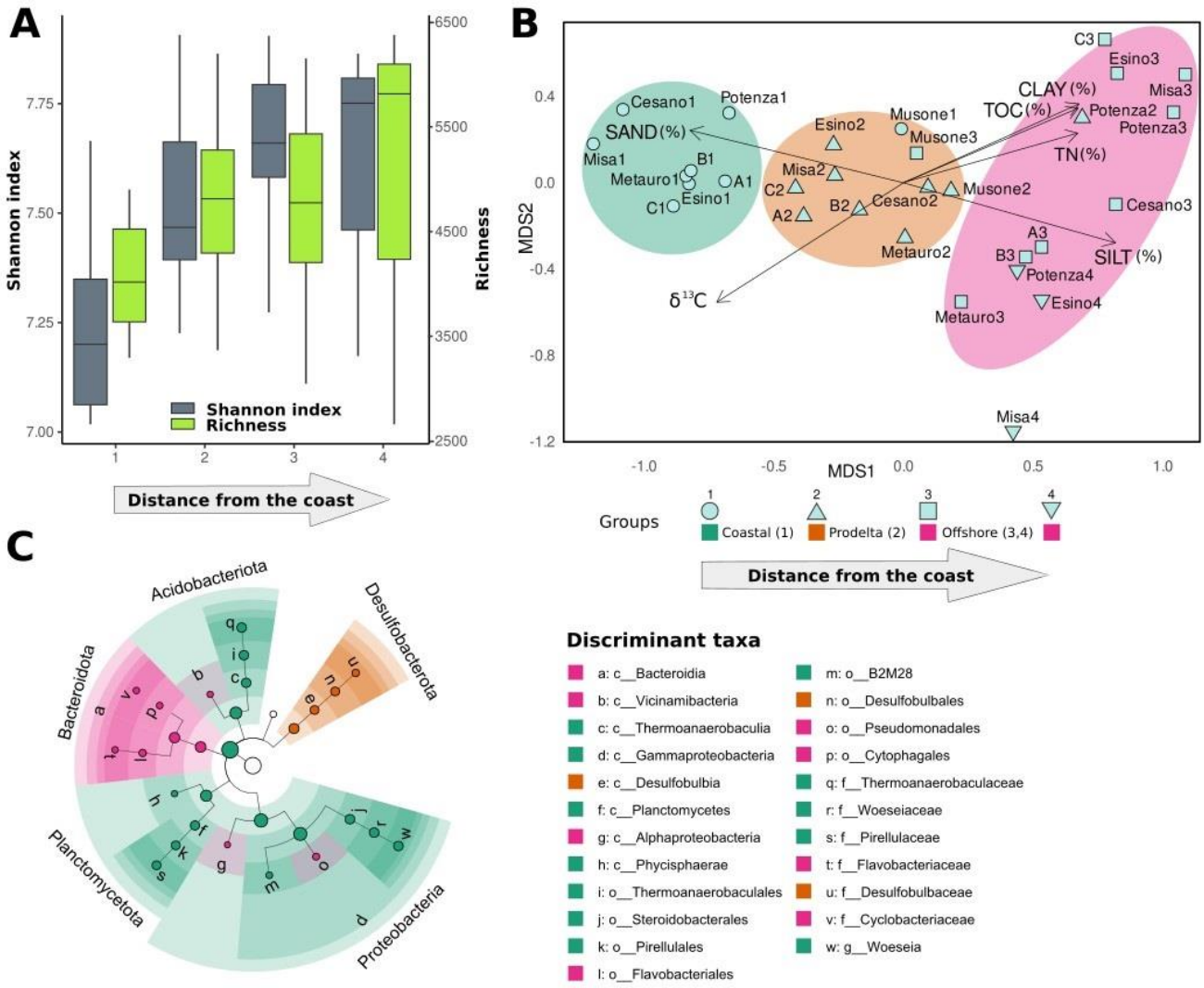

Figure 10: Microbial community structure and diversity across the coast-to-sea transects in river flood sediments deposited in 2022. (A) Boxplots of Shannon diversity and Amplicon Sequence Variant (ASV) richness indices, clustered by distance from the coast and river impact. (B) Non-metric Multidimensional Scaling (nMDS) ordination based on a Bray-Curtis dissimilarity matrix (Stress = 0.20); shapes indicate distance clusters, and ellipses represent 95% confidence intervals; TOC: Total Organic Carbon; TN: Total Nitrogen. (C) Linear discriminant analysis Effect Size (LEfSe) cladogram showing differentially abundant taxa ($p < 0.001$) among clusters from the nMDS; each dot represents a discriminant taxon, colored by the cluster in which it is most abundant.

5. DISCUSSION

~~The sedimentological sampling of the coastal, prodelta, and offshore regions after a major flood event, impacting a very small catchment, documents how physical transport processes directly modulate chemical and biological responses in this interconnected system through fine-grained sediment, combined with short-distance shifts in microbial community composition. This integrative framework, synthesized in figure 11, enables a more holistic understanding of the short-term sedimentary and ecological responses to a river flood seen as an extreme hydrological disturbance. In this framework, the dispersal of fine-grained flood deposits is the primary physical forcing on contaminant redistribution and biological responses.~~ To provide a unified interpretation of the physical, geochemical, and microbiological patterns described above, we developed a conceptual framework that links the three major process domains addressed in the Discussion. First, meteo-oceanographic forcing controls whether flood-derived sediments are bypassed nearshore or temporarily accumulated in the prodelta (Section 5.1). Second, pollutant distribution reflects the different transport pathways characterizing each contaminant class, with PAHs largely following fine-grained sediment transport and PFASs exhibiting patterns shaped by fluvial–marine water mixing (Section 5.2) Third, the sediment heterogeneity shapes benthic microbial community structure, producing distinct coastal, prodelta, and offshore assemblages (Section 5.3). Figure 11 summarizes these coupled processes along a cross-shore transect, illustrating how a single flood event simultaneously drives sediment transport, contaminant hotspots, and microbial community shifts.

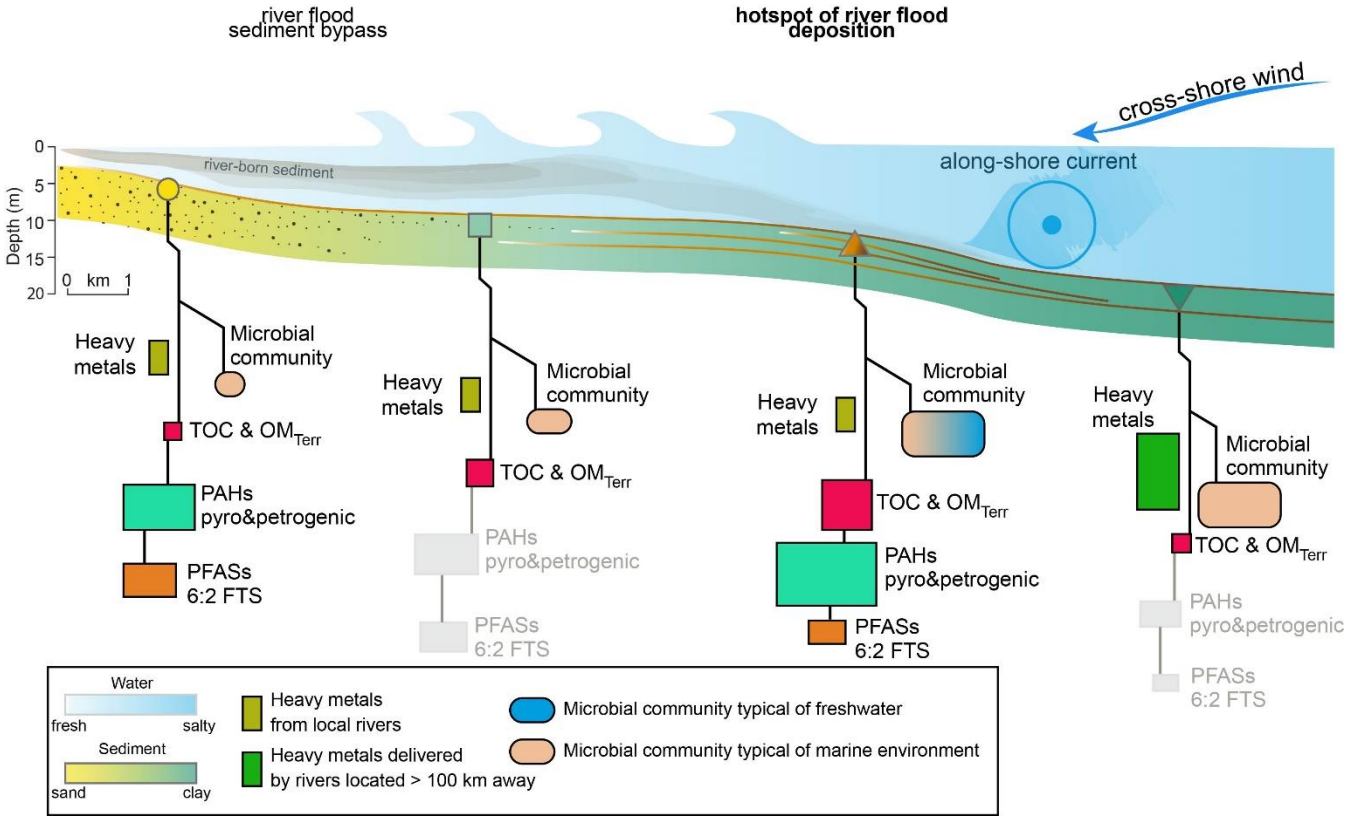

Figure 11: Conceptual model of sediment transport, contaminant distribution, and microbial community variation along a coastal transect where sediment and associated contaminants are transported and deposited across a coastal gradient under the influence of riverine input, wave action, and along-shelf currents. During flood events, high-energy river flows can bypass the wave-influenced coastal zone and deliver sediments offshore, where they are preferentially deposited in the prodelta. This distal accumulation occurs in areas where the energy of the plume is reduced, and flow is laterally confined by the prevailing along-shelf current.

The size of the shapes reflects the relative abundance of each contaminant class (PAHs: Polycyclic Aromatic Hydrocarbons; PFASs: Poly- and Perfluorinated alkyl substances), while the size of the microbial community symbol reflects diversity rather than quantity. Colors differentiate sources (e.g., local vs. remote rivers) and environmental

influences (e.g., fresh vs. salt water). TOC: Total Organic Carbon; OM_{Terr}: Terrigenous Organic Matter; FTS: fluorotelomer sulfonate.

410

5.1 Meteorological-oceanographic controls on river flood deposits

The spatial distribution and preservation of the September 2022 flood deposit is controlled by the interplay between fluvial input and coastal meteo-oceanographic dynamics (Fig. 11). Depositional processes govern sediment transport pathways, and grain size distribution with finer sediments prevailing in the prodelta, and coarser sediments in the coastal zones subject to
415 occasional resuspension. Further nearshore (in less than ~5 m water depth) adjacent to river mouths, sediment retention is hampered by intense wave-induced resuspension and alongshore transport driven by coastal currents. In the case of the September 2022 flood event, the rapid intensification of northeasterly winds during the final phase of the flooding intensified cross shore sea state and alongshore currents (Fig. 2), increasing bed shear stresses, and leading to remobilization of flood-derived sediments. The sandy nearshore sector is therefore subject to continuous remobilization and winnowing, with a
420 persistent southward advection of river-derived sediment plumes, in agreement with previous findings (Palinkas and Nittrouer, 2006; Cattaneo et al., 2007; Fain et al., 2007; Friedrichs and Scully, 2007; Puig et al., 2007; Traykovski et al., 2007; Pellegrini et al., 2024). As a result, the nearshore zone acts as a high-energy bypass area where sedimentary, chemical, and biological flood signals are rapidly blurred (Fig. 11).

In contrast, further distal prodelta environments (at ca. 10-15 m water depth) provide more favorable conditions for
425 preservation of flood deposits (Fig. 11). Here, sedimentary features such as rip-up clasts of semi-consolidated mud, together with an enrichment in terrigenous organic carbon, indicate the deposition of fine sediments that were previously eroded at the river mouth and subsequently bypassed and redeposited in the prodelta. These processes resemble the depositional patterns of river-borne sediments emplaced close to the river mouth, which typically undergo only limited transport distance and short residence time during their seaward transfer (Pellegrini et al., 2021, 2024). Hydrodynamics model and *in-situ* data support this
430 interpretation, showing a rapid but transient intensification of coastal currents in response to the windstorm, suggestive of dynamic interactions between river discharge and marine hydrodynamics over timescales of just hours. Similar sediment transport and current patterns linked to northeasterlies (locally known as Bora winds) and the Western Adriatic Coastal Current

(WACC) have been documented in previous studies (Wang and Pinardi, 2002; Sherwood et al., 2004; Book et al., 2007; Palinkas et al., 2007; Harris et al., 2008; Signell et al., 2010; Benincasa et al., 2019; Vona et al., 2025). On the other hand, the short duration of the windstorm most likely limited southward sediment displacement, effectively trapping suspended particles within the prodelta and causing a spatially restricted, temporary accumulation of river-derived material (Fig. 11). This effect is particularly evident for the Misa River, the smallest of the six adjacent drainage systems, characterized by reduced channel sinuosity, which limits onland sediment storage and promotes rapid offshore transport. The exceptional impact of the September 2022 flood was driven by the persistence of an intense precipitation cell over this very small catchment for several hours (Fig. 1). This evidence demonstrates that even extreme flood events of small "dirty-river" catchments like that of Misa and adjacent small rivers, can leave only elusive stratigraphic signals in inner shelf records, raising concerns about detecting high-magnitude river floods in modern marine sedimentary records.

Finally, samples collected farther offshore and unaffected by the September 2022 flood show sediment compositions attributable to the Western Alps (Amorosi et al., 2022 for a review), indicating that river-borne sediment was hydrodynamically confined by the WACC during the event (Fig. 11).

5.2 Pollutant distribution patterns reflecting fluvial and oceanographic processes

Understanding the origin and behavior of contaminants in marine sediments is crucial for assessing risks to the environment and to human-health and, more in general, for implementing effective coastal management strategies (Neff et al., 2005; Di Lorenzo et al., 2020; Pizzini et al., 2021; Pellegrini et al., 2023; Trincardi et al., 2023). Given the hydrodynamic confinement and selective deposition processes described above, contaminant distributions following flood events are expected to be spatially heterogeneous rather than uniformly dispersed. In this study, the spatial heterogeneity of sediment-bound contaminants reflects differential transport and depositional pathways shaped by sediment dynamics and chemical properties (Fig. 11).

PAHs, which are largely associated with the particulate phase, showed enhanced offshore dispersal following the flood event, with elevated concentrations in prodelta areas influenced by riverine plumes (Figs. 7, 11). This apparent offshore redistribution does not imply increased chemical mobility but rather reflects the efficient transport of PAH-bearing fine particles during

flood-driven sediment dispersal. This redistribution is consistent with the deposition of fine-grained, organic-rich sediments characterized by $\delta^{13}C$ signatures indicative of a predominantly terrigenous origin (Tesi et al., 2007; Bao et al., 2016; Bröder et al., 2018; Hage et al., 2022; Nogarotto et al., 2023). These sediments act as efficient carriers for hydrophobic organic contaminants, including PAHs. The grain-size dependence of PAH distribution and their strong positive correlation with TOC likely reflect the preferential sorption of PAHs onto natural organic matter (Hedges and Keil, 1999; Bucheli et al., 2004; Lohmann et al., 2005; Stout and Emsbo-Mattingly, 2008; Ukalska-Jaruga et al., 2018). The close correspondence between PAH concentrations and TOC has been widely documented in both marine and terrestrial sediments (Soclo et al., 2000; Rockne et al., 2002; Talley et al., 2002; Vane et al., 2007, 2020; Nascimento et al., 2017).

Consistently, PAH concentrations display a positive correlation with fine sediment fractions (clay and silt), while sand content is negatively correlated. This relationship may arise from PAHs being partitioned onto organic matter coatings associated with clay and silt particles and/or through direct adsorption onto clay mineral surfaces. In this context, organic matter behaves hydrodynamically similarly to the fine-grained fraction, facilitating the coupled transport and deposition of PAHs with clay-rich sediments during flood-driven dispersal. This suggests that hydrophobic organic contaminants follow the transport dynamics of organic-rich riverine clays, similar to other prodelta systems (Roussiez et al., 2006; Bouloubassi et al., 2012). During flood events, the rapid delivery of fine-grained, organic-rich material enhances the efficiency of PAH transport by coupling contaminant partitioning with hydrodynamic sorting. This process promotes the selective offshore focusing of PAHs at the prodelta where fine sediments and organic matter accumulate (Fig. 11). Indeed, the Adriatic prodelta deposits, especially near the Misa River, show PAH concentrations up to five times higher than coastal samples, creating localized pollutant hotspots of significant environmental concern (Fig. 11). Moreover, the spatial distribution of PAHs is heterogeneous and shaped by both diffuse and point sources, with elevated concentrations near urban and industrial centers such as Fano, Senigallia, and Ancona. These areas are influenced by harbor activities, vehicular traffic, and maritime transport (Frapiccini et al., 2024). Even mountainous areas, typically less impacted by anthropogenic activity, present detectable PAH levels, likely linked to fossil fuel combustion for domestic heating during winter. This demonstrates that short-lived flood events can generate spatially concentrated contaminant accumulation with potentially disproportionate ecological relevance.

In contrast, PFASs showed a distinct spatial pattern due to their chemical properties, displaying limited offshore dispersion regardless of sediment grain size, reflecting the complexity of contaminant-sediment interactions influenced by granulometry and chemical affinities and with highest concentrations confined near river mouths (Fig. 9, 11). This pattern highlights a key difference in transport mechanisms: PFASs, unlike traditional Persistent Organic Pollutants (POPs), are not primarily governed by sorption onto organic matter. Their surfactant-like properties and amphiphilic structure cause them to interact distinctively with saline environments through processes such as the salting-out effect, which reduces their solubility as salinity increases, limiting offshore transport (Pan and You, 2010; Jeon et al., 2011; Wang et al., 2013; Munoz et al., 2017; Newell et al., 2022; Steffen et al., 2021; Li et al., 2022; Yin et al., 2022; Hort et al., 2024). This is evident in the 2022 flood event, where PFAS distribution was influenced by mixing of freshwater flood plumes with marine waters, resulting in preferential accumulation near the coast (Fig. 11).

Deeper sediment layers deposited prior to the 2022 flood showed minimal PFAS concentrations, with trace amounts of 6:2 FTS detected in northern transects (A, Metauro River, B, and Cesano River), suggesting historical contamination potentially linked to earlier flood events. Surface sediments associated with the 2022 flood revealed 6:2 FTS as the dominant compound, followed by 8:2 FTS, reflecting the influence of newer-generation PFASs used as alternatives to banned legacy compounds (Field and Seow, 2017). Traditional PFASs such as PFHxA, PFOA, and PFUnA were widespread, with peak concentrations offshore of the Misa River, confirming Senigallia as a primary hotspot. Elevated PFAS levels were also recorded in the Metauro River transect, likely due to upstream industrial activities such as non-stick cookware manufacturing. Higher Cu concentrations in these sediments corroborate anthropogenic pressure, although values remained below regulatory limits (120 mg kg^{-1}). This area remains under active environmental monitoring by regional agencies (e.g., ARPAM: The Marche Regional Environmental Protection Agency). In contrast, the absence of PFAS contamination in sediments collected South of the Ancona Promontory is likely related to the lack of significant point and diffuse sources within the Musone and Potenza river catchments, which are not characterized by major industrial activities typically associated with these compounds. Additionally, local coastal hydrodynamics may have played a key role, as WACC and the related nearshore confinement processes could have constrained contaminant transport, promoting the retention of riverine inputs upstream of Ancona Promontory and limiting their deposition in the investigated sector.

In summary, the spatial and compositional variability of pollutants observed in this study underscores the importance of event-based monitoring strategies. While the 2022 flood had a broad hydrodynamic impact, its contaminant impact was spatially selective, reinforcing pre-existing gradients rather than creating a uniformly distributed pollution layer. PAHs were redistributed more broadly due to their particulate-bound nature, whereas PFASs remained concentrated near-source due to their solubility and surfactant behavior (Fig. 11). These findings highlight the complex interplay between sediment dynamics and contaminant chemistry in shaping pollutant distribution following extreme river flood events, with important implications for coastal ecosystem management and resilience.

Finally, the preferential accumulation of flood-transported sediments and associated pollutants at the 10–15 m isobath creates distinct biogeochemical "hotspots" or pollutant sinks within the prodelta environment (Fig. 11). This pattern of spatial segregation highlights the need to focus monitoring and remediation efforts on these depositional zones, which play a crucial role in controlling contaminant cycling and storage in coastal systems.

5.3 Flood-derived sedimentation as a driver of benthic microbial community structure

To explore the distribution of the September 2022 flood, we analyzed samples along a coastal-to-offshore transect. This analysis was designed to identify spatial associations rather than infer direct causality between flood forcing and microbial community change. Overall, our integrated microbial, sedimentological, and geochemical approach revealed that the 2022 flood triggered a selective reorganization of benthic communities. The observed increase in microbial diversity with increasing distance from shore generally reflected the presence of finer sediments and decreasing physical disturbance offshore, along the transect (Fig. 11). Coastal sites, with coarser sediments, elevated levels of PAHs and PFASs, and stronger wave disturbance, exhibited significantly lower microbial diversity, consistent with other coastal systems where physical stress and exposure to pollutantants was associated with reduced richness and functional complexity (Quero et al., 2015; Cibic et al., 2019). Offshore assemblages were more diverse and taxonomically heterogeneous, forming subclusters associated with fine-grained, TOC- and TN-enriched sediments typical of flood deposits. The spatial overlap of fine-grained flood deposits, localized contaminant hotspots (notably PAHs and PFASs), and distinct microbial communities underscores the tight coupling between sediment transport and biogeochemical functioning. Fine sediments act as vectors for hydrophobic contaminants,

concentrating pollutants in depositional hotspots such as the prodelta at 10–15 m water depth, which serve as key pollutant sinks. These environments may thus favor microbial assemblages adapted to organic-rich and contaminated conditions, including freshwater-derived taxa indicative of recent riverine inputs (Fig. 11). Both microbial community structure and the analysis of biomarker taxa revealed distinct communities associated, respectively, with coastal, prodelta, and offshore stations; the taxa driving these differences are linked to riverine or marine sedimentary environments (Fig. 10c). The presence of freshwater-indicator taxa (Flavobacteriaceae, Vicinamibacteria, Comamonadaceae) supports the hypothesis of a direct riverine influence on offshore communities, aligning with previous findings on flood-driven dispersal (Giner-Lamia et al., 2024; Massaccesi et al., 2025). Moreover, the spatial confinement of these "flood-influenced" microbial signatures reflects physical sediment transport limits imposed by meteo-oceanographic conditions. The northeasterly storm following the flood enhanced offshore transport of fine particles while restricting their dispersion beyond the 15 m isobath, shaping both sedimentary and biological patterns (Fig. 11). Thus, hydrodynamic processes not only regulate sediment and contaminant dispersal, but it might also indirectly affect microbial community assemblages' diversity and functioning (Voynova et al., 2017; Fazi et al., 2020; Steichen et al., 2020; Jajun et al., 2024; Vona et al., 2025).

Overall, our findings suggest that, despite the transient nature of flood sediment deposits, flood-driven sediment dynamics may directly shape benthic microbial communities by delivering distinct sediment types and associated contaminants, and that ecologically meaningful shifts in benthic ecosystem functioning can occur. Taking together, these spatially constrained patterns raise the broader question of how increasingly frequent or intense flood events may translate into persistent, long-term changes in coastal ecosystems. Although limited, available post-flood studies consistently indicate that repeated flood-driven inputs alter coastal carbon and nutrient budgets as well as oxygen dynamics over seasonal to multiannual timescales (Sommerfield and Nittrouer, 1999; Geyer et al., 2000; Drexler and Nittrouer, 2008; Tesi et al., 2013; Steichen et al., 2020). The magnitude, direction, and possible recovery of these biological and biogeochemical shifts in response to recurrent exposure to such perturbations emphasizes the need for integrated, long-term event-focused monitoring coupling microbial and geochemical data, particularly in regions prone to frequent extreme hydrological events.

CONCLUSIONS

Despite its severe onland impact, the September 2022 river flood left a transient and spatially heterogeneous sedimentary record offshore, highlighting the extent to which meteo-oceanographic conditions control the distribution of sediments, contaminants, and benthic microbial communities. The sandy coastal zone experienced intense wave- and current-driven resuspension and alongshore transport, limiting the accumulation and preservation of flood-derived sediment. In contrast, fluvial inputs were largely confined to the prodelta, where reduced wave-induced shear stress enabled the temporary deposition of fine-grained material. Strong Bora-driven hydrodynamics further prevented offshore dispersal beyond the 15 m isobath. Thus, despite the flood's major inland impact, the resulting offshore deposit remained patchy and ephemeral, leaving a sedimentary signal that is difficult to preserve in the marine stratigraphic record.

The 2022 flood also redistributed both traditional and emerging contaminants. Analyses of PAHs and PFASs reveal a complex interplay between chronic anthropogenic pressures and episodic hydrological events. PAHs, predominantly associated with fine organic particles, exhibited wider offshore transport following the flood, whereas PFASs remained concentrated near river mouths due to their distinct physicochemical properties. These contrasting behaviours highlight the importance of targeted monitoring strategies in industrialized and flood-prone coastal systems, such as the Misa River area, where contaminant concentrations and mobility can vary substantially during extreme events.

Flood-induced sediment heterogeneity was also reflected in the structure of benthic microbial assemblages. Coarse, sandy coastal substrates hosted lower-diversity communities dominated by taxa such as *Thermoanaerobaculaceae* and *Woeseiaceae*, indicative of elevated physical disturbance and contaminant exposure. Conversely, fine-grained, organic-rich prodelta deposits supported more diverse prokaryotic assemblages, including freshwater-derived taxa linked to direct riverine input. Over decadal timescales, the cumulative effect of repeated ephemeral depositional events has the potential to induce lasting shifts in coastal biogeochemical cycles and benthic ecosystem structure.

Overall, this study underscores the value of multidisciplinary approaches in resolving coastal responses to extreme hydrological events. By integrating sediment transport dynamics, hydrodynamics, microbial ecology, and contaminant behavior, we provide a more comprehensive understanding of how river floods modulate the land-sea interface. Recognizing the ephemeral yet impactful nature of these events is essential not only for interpreting recent sedimentary records but also for anticipating future environmental trajectories in the Mediterranean and other climatically sensitive coastal systems.

DATA AVAILABILITY

All data supporting the findings of this study are provided within the article and its Supplementary Material, or are available from the authors upon request.

COMPETING INTERESTS

The authors declare that they have no conflict of interest.

AUTHOR CONTRIBUTIONS

CP: Conceptualization, co-design of the survey; oceanographic survey activity; sedimentological analyses; data integration; figure preparation; writing original draft; funding acquisition. MB: Oceanographic survey activity; sampling and bacterial analyses; figure preparation; writing, review and editing. IS: Geochemical analyses and interpretation; figure preparation; data curation, writing, review and editing. TT: Co-designed the survey, oceanographic survey activity; organic matter characterization; review and editing. EF: PAH analyses; writing, review and editing. GMQ: bacterial analysis, interpretation, and writing. SP: PFAS analyses, interpretation, writing, review and editing. RZ: PFAS analyses. GML: institutional and infrastructural support for the survey; review and editing. SC: Sedimentological analyses. BC: Sedimentological analyses. NM: Oceanographic survey activity; sampling and bacterial analyses; review and editing. FT: Proposed the survey; review and editing. AG: Oceanographic survey activity. JC: Meteo-oceanographic data curation; interpretation; writing, review and editing.

ACKNOWLEDGMENTS

This project has received funding from the Italian Ministry of University and Research under the PRIN (National Interest Research Project) ON-OFF - Project contract 2022PMEN2K, and from EU - NextGenerationEU, Mission 4, Component 2 - CUP B53C22002150006 - Project IR0000032 – ITINERIS – Italian Integrated Environmental Research Infrastructures

System. The authors want to thank the Editor, Sebastian Naeher, for the constructive editorial guidance as well as Rui Bao, Mengfan Chu, and the anonymous Reviewer for their constructive comments and discussions that helped to improve manuscript readability. The authors also thank Silvio Davolio (CNR-ISAC), Pierluigi Penna (CNR-IRBIM), and Silvia Unguendoli (ARPAE) for, respectively, MOLOCH, TeleSenigallia, and Adriac data provision. Federico Falcini (CNR-ISMAR) is thankful for sharing orthophoto images. Professor Juergen Schieber is thanked for his support in sediment samples impregnation. Finally, thanks to ELGA LabWater (Veolia Water VWS Ltd., High Wycombe, UK) for supplying the PURELAB® systems used in this study during the PFAS analysis.

REFERENCES

Adeoba, M. I., Pandelani, T., Ngwangwa, H., and Masebe, T.: The Role of Artificial Intelligence in Sustainable Ocean Waste Tracking and Management: A Bibliometric Analysis, Sustainability, 17, 3912, https://doi.org/10.3390/su17093912, 2025.

Ainsworth, R. B., Vakarelov, B. K., and Nanson, R. A.: Dynamic spatial and temporal prediction of changes in depositional processes on clastic shorelines: toward improved subsurface uncertainty reduction and management, AAPG Bull., 95, 267–297, https://doi.org/10.1306/06301010036, 2011.

Allan, R. P. and Soden, B. J.: Atmospheric warming and the amplification of precipitation extremes, Science, 321, 1481–1484, DOI: 10.1126/science.1160787, 2008.

Amorosi, A. and Sammartino, I.: Influence of sediment provenance on background values of potentially toxic metals from near-surface sediments of Po coastal plain (Italy), Int. J. Earth Sci., 96, 389–396, https://doi.org/10.1007/s00531-006-0104-8, 2007.

Amorosi, A., Guermandi, M., Marchi, N., and Sammartino, I.: Fingerprinting sedimentary and soil units by their natural metal contents: a new approach to assess metal contamination, Sci. Total Environ., 500, 361–372, https://doi.org/10.1016/j.scitotenv.2014.08.078, 2014.

Amorosi, A., Sammartino, I., Dinelli, E., Campo, B., Guercia, T., Trincardi, F., and Pellegrini, C.: Provenance and sediment dispersal in the Po-Adriatic source-to-sink system unraveled by bulk-sediment geochemistry and its linkage to catchment geology, Earth-Sci. Rev., 234, 104202, https://doi.org/10.1016/j.earscirev.2022.104202, 2022.

Anthony, E. J., Marriner, N., and Morhange, C.: Human influence and the changing geomorphology of Mediterranean deltas and coasts over the last 6000 years: From progradation to destruction phase?, Earth-Sci. Rev., 139, 336–361, https://doi.org/10.1016/j.earscirev.2014.10.003, 2014.

Anthony, E., Syvitski, J., Zăinescu, F., Nicholls, R. J., Cohen, K. M., Marriner, N., and Maselli, V.: Delta sustainability from the Holocene to the Anthropocene and envisioning the future, Nat. Sustain., 7, 1235–1246, https://doi.org/10.1038/s41893-024-01426-3, 2024.

Arienzo, M., Donadio, C., Mangoni, O., Bolinesi, F., Stanislao, C., Trifuoggi, M., Toscanesi, M., Di Natale, G., and Ferrara, L.: Characterization and source apportionment of polycyclic aromatic hydrocarbons (PAHs) in the sediments of Gulf of Pozzuoli (Campania, Italy), Mar. Pollut. Bull., 124, 480–487, https://doi.org/10.1016/j.marpolbul.2017.07.006, 2017.

Bao, R., McIntyre, C., Zhao, M., Zhu, C., Kao, S. J., and Eglinton, T. I.: Widespread dispersal and aging of organic carbon in shallow marginal seas, Geology, 44, 791–794, DOI: 10.1130/G37948.1, 2016.

Bao, R., van der Voort, T. S., Zhao, M., Guo, X., Montluçon, D. B., McIntyre, C., and Eglinton, T. I.: Influence of hydrodynamic processes on the fate of sedimentary organic matter on continental margins, Global Biogeochem. Cycles, 32, 1420–1432, https://doi.org/10.1029/2018GB005921, 2018.

Basili, M., Campanelli, A., Frapiccini, E., Luna, G. M., and Quero, G. M.: Occurrence and distribution of microbial pollutants in coastal areas of the Adriatic Sea influenced by river discharge, Environ. Pollut., 285, 117672, https://doi.org/10.1016/j.envpol.2021.117672, 2021.

Benincasa, M., Falcini, F., Adduce, C., Sannino, G., and Santoleri, R.: Synergy of satellite remote sensing and numerical ocean modelling for coastal geomorphology diagnosis, Remote Sens., 11, 2636, https://doi.org/10.3390/rs11222636, 2019.

Bentley, S. J. and Nittrouer, C. A.: Emplacement, modification, and preservation of event strata on a flood-dominated continental shelf: Eel shelf, Northern California, Cont. Shelf Res., 23, 1465–1493, https://doi.org/10.1016/j.csr.2003.08.005, 2003.

Bentley, S. J., Sheremet, A., & Jaeger, J. M.: Event sedimentation, bioturbation, and preserved sedimentary fabric: field and model comparisons in three contrasting marine settings. Continental Shelf Research, 26(17-18), 2108-2124, https://doi.org/10.1016/j.csr.2006.07.003, 2006.

Bhattacharya, J. P. and MacEachern, J. A.: Hyperpycnal rivers and prodeltaic shelves in the Cretaceous seaway of North America, J. Sediment. Res., 79, 184–209, https://doi.org/10.2110/jsr.2009.026, 2009.

Bianchi, T. S., Morrison, E., Barry, S., Arellano, A. R., Feagin, R. A., Hinson, A., and Oviedo-Vargas, D.: The fate and transport of allochthonous blue carbon in divergent coastal systems, in: A blue carbon primer, CRC Press, 27–49, 2018.

Blair, N. E., and Aller, R. C.: The fate of terrestrial organic carbon in the marine environment. Annual review of marine science, 4, 401-423, https://doi.org/10.1146/annurev-marine-120709-142717, 2012.

Blöschl, G. and Grayson, R.: Spatial observations and interpolation, in: *Spatial Patterns in Catchment Hydrology: Observations and Modelling*, edited by: Grayson, R. and Blöschl, G., Cambridge University Press, Cambridge, UK, 13–16, 2000.

Blöschl, G., Hall, J., Parajka, J., Perdigão, R. A., Merz, B., Arheimer, B., and Živković, N.: Changing climate shifts timing of European floods, Science, 357, 588–590, DOI: 10.1126/science.aan2506, 2017.

Blott, S. J. and Pye, K.: GRADISTAT: a grain size distribution and statistics package for the analysis of unconsolidated sediments, Earth Surf. Process. Landforms, 26, 1237–1248, https://doi.org/10.1002/esp.261, 2001.

Blum, M. D. and Roberts, H. H.: Drowning of the Mississippi Delta due to insufficient sediment supply and global sea -level rise, Nat. Geosci., 2, 488–491, https://doi.org/10.1038/ngeo553, 2009.

Bolan, L. P., Padhye, T., Jasemizad, M., Govarthanan, M., Karmegam, N., Wijesekara, H., Amarasiri, D., Hou, D., Zhou, P., Biswal, B. K., Balasubramanian, R., Wang, H., Siddique, K. H. M., Rinklebe, J., Kirkham, M. B., and Bolan, N.: Impacts of climate change on the fate of contaminants through extreme weather events, Sci. Total Environ., 909, 168388, https://doi.org/10.1016/j.scitotenv.2023.168388, 2024.

Book, J. W., Signell, R. P., and Perkins, H.: Measurements of storm and nonstorm circulation in the northern Adriatic: October 2002 through April 2003, J. Geophys. Res., 112, C11S92, https://doi.org/10.1029/2006JC003556, 2007.

Bosman, A., Romagnoli, C., Madricardo, F., Correggiari, A., Remia, A., Zubalich, R., and Trincardi, F.: Short -term evolution of Po della Pila delta lobe from time lapse high-resolution multibeam bathymetry (2013–2016), Estuar. Coast. Shelf Sci., 233, 106533, https://doi.org/10.1016/j.ecss.2019.106533, 2020.

Bouloubassi, I., Roussiez, V., Azzoug, M., and Lorre, A.: Sources, dispersal pathways and mass budget of sedimentary polycyclic aromatic hydrocarbons (PAH) in the NW Mediterranean margin, Gulf of Lions, Mar. Chem., 142, 18–28, https://doi.org/10.1016/j.marchem.2012.07.003, 2012.

Bröder, L., Tesi, T., Andersson, A., Semiletov, I., Dudarev, O., Gustafsson, Ö., and Eglinton, T. I.: Bounding cross-shelf transport time and degradation in Siberian–Arctic land–ocean carbon transfer, Nat. Commun., 9, 806, https://doi.org/10.1038/s41467-018-03192-1, 2018.

Bucheli, T. D., Blum, F., Desaules, A., and Gustafsson, Ö.: Polycyclic aromatic hydrocarbons, black carbon, and molecular markers in soils of Switzerland, Chemosphere, 56, 1061–1076, https://doi.org/10.1016/j.chemosphere.2004.04.015, 2004.

Bue, G. L., Musa, M., Marchini, A., Riccardi, M. P., Dubois, S. F., Lisco, S., and Mancin, N.: Microplastic pollution in the littoral environment: insights from the largest Mediterranean Sabellaria spinulosa (Annelida) reef and shoreface sediments, Mar. Pollut. Bull., 217, 118132, https://doi.org/10.1016/j.marpolbul.2025.118132, 2025.

Callahan, B. J., McMurdie, P. J., Rosen, M. J., Han, A. W., Johnson, A. J. A., and Holmes, S. P.: DADA2: High-resolution sample inference from Illumina amplicon data, Nat. Methods, 13, 581–583, https://doi.org/10.1038/nmeth.3869, 2016.

Campanelli, A., Grilli, F., Paschini, E., and Marini, M.: The influence of an exceptional Po River flood on the physical and chemical oceanographic properties of the Adriatic Sea, Dyn. Atmos. Oceans, 52, 284–297, https://doi.org/10.1016/j.dynatmoce.2011.05.004, 2011.

Cattaneo, A., Trincardi, F., Asioli, A., and Correggiari, A.: The late-Holocene Gargano subaqueous delta, Adriatic shelf: sediment pathways and supply fluctuations, Mar. Geol., 193, 61–91, https://doi.org/10.1016/S0025-3227(02)00613-5, https://doi.org/10.1016/S0025-3227(02)00614-X, 2003.

Cattaneo, A., Trincardi, F., Asioli, A., and Correggiari, A.: The Western Adriatic shelf clinoform: energy-limited bottomset, Cont. Shelf Res., 27, 506–525, https://doi.org/10.1016/j.csr.2006.11.013, 2007.

Cecchetto, M., Giubilato, E., Bernardini, I., Bettiol, C., Asnicar, D., Bertolini, C., and Semenzin, E.: A Weight of Evidence approach to support the assessment of the quality of Manila clam farming sites in a coastal lagoon. Marine Pollution Bulletin, 197, 115668, https://doi.org/10.1016/j.marpolbul.2023.115668, 2023.

Cecchi, G., Cutroneo, L., Di Piazza, S., Besio, G., Capello, M., and Zotti, M.: Port sediments: problem or resource? A review concerning the treatment and decontamination of port sediments by fungi and bacteria, Microorganisms, 9, 1279, https://doi.org/10.3390/microorganisms9061279, https://doi.org/10.3390/microorganisms9061279, 2021.

Chen, J., Yu, Z., Gao, X., Zhang, J., Lin, J., and Wei, Y.: Bacterial communities in riparian sediments: a large-scale longitudinal distribution pattern and response to dam construction, Front. Microbiol., 9, 999, https://doi.org/10.3389/fmicb.2018.00999, https://doi.org/10.3389/fmicb.2018.00999, 2018.

Cibic, T., Fazi, S., Nasi, F., Pin, L., Alvisi, F., Berto, D., and Del Negro, P.: Natural and anthropogenic disturbances shape benthic phototrophic and heterotrophic microbial communities in the Po River Delta system, Estuar. Coast. Shelf Sci., 222, 168–182, https://doi.org/10.1016/j.ecss.2019.04.009, 2019.

Clark, D. R., Underwood, G. J. C., McGenity, T. J., and Dumbrell, A. J.: What drives study-dependent differences in distance–decay relationships of microbial communities?, Glob. Ecol. Biogeogr., 30, 811–825, https://doi.org/10.1111/geb.13266, 2021.

Cohen, S., Syvitski, J., Ashley, T., Lammers, R., Fekete, B., and Li, H. Y.: Spatial trends and drivers of bedload and suspended sediment fluxes in global rivers, Water Resour. Res., 58, e2021WR031583, https://doi.org/10.1029/2021WR031583, 2022.

Coleman, J. M. and Wright, L. D.: Modern river deltas: variability of processes and sand bodies, Houston Geological Society, 99–149, 1975.

Danovaro, R., Corinaldesi, C., Dell'Anno, A., and Rastelli, E.: Potential impact of global climate change on benthic deep-sea microbes, FEMS Microbiol. Lett., 364, fnx214, https://doi.org/10.1093/femsle/fnx214, 2017.

Death, R. G., Fuller, I. C., & Macklin, M. G.: Resetting the river template: The potential for climate-related extreme floods to transform river geomorphology and ecology. Freshwater Biology, 60(12), 2477-2496, https://doi.org/10.1111/fwb.12639, 2015.

De Lucia, C., Amaddii, M., and Arrighi, C.: Tangible and intangible ex post assessment of flood-induced damage to cultural heritage, Nat. Hazards Earth Syst. Sci., 24, 4317–4339, https://doi.org/10.5194/nhess-24-4317-2024, 2024.

DesRosiers, A., Gassama, N., Grosbois, C., and Lazar, C. S.: Laboratory-controlled experiments reveal microbial community shifts during sediment resuspension events, Genes, 13, 1416, https://doi.org/10.3390/genes13081416, 2022.

Di Lorenzo, T., Hose, G. C., and Galassi, D. M. P.: Assessment of different contaminants in freshwater: origin, fate and ecological impact, Water, 12, 1810, https://doi.org/10.3390/w12061810, 2020.

Dinelli, E., Lucchini, F., Mordenti, A., and Paganelli, L.: Geochemistry of Oligocene–Miocene sandstones of the northern Apennines (Italy) and evolution of chemical features in relation to provenance changes, Sediment. Geol., 127, 193–207, https://doi.org/10.1016/S0037-0738(99)00049-4, 1999.

Donnini, M., Santangelo, M., Gariano, S. L., Bucci, F., Peruccacci, S., Alvioli, M., and Fiorucci, F.: Landslides triggered by an extraordinary rainfall event in Central Italy on 15 September 2022, Landslides, 20, 2199–2211, https://doi.org/10.1007/s10346-023-02061-4, 2023.

Dottori, F., Mentaschi, L., Bianchi, A., Alfieri, L., and Feyen, L.: Cost-effective adaptation strategies to rising river flood risk in Europe, Nat. Clim. Chang., 13, 196–202, https://doi.org/10.1038/s41558-022-01581-0, 2023.

Drexler, T. M. and Nittrouer, C. A.: Stratigraphic signatures due to flood deposition near the Rhône River: Gulf of Lions, northwest Mediterranean Sea, Cont. Shelf Res., 28, 1877–1894, https://doi.org/10.1016/j.csr.2007.11.012, 2008.

Ennas, C., Pasquini, V., Addis, P., and Pusceddu, A.: Short-term effects of a simulated massive river flood and its recovery on sediment biogeochemistry of a Mediterranean lagoon. *Chemistry and Ecology*, *40*(5), 487-500, https://doi.org/10.1080/02757540.2024.2338178, 2024.

Fain, A. M. V., Ogston, A. S., and Sternberg, R. W.: Sediment transport event analysis on the western Adriatic continental shelf, Cont. Shelf Res., 27, 431–451, https://doi.org/10.1016/j.csr.2005.03.007, 2007.

Falcini, F., Khan, N. S., Macelloni, L., Horton, B. P., Lutken, C. B., McKee, K. L., and Jerolmack, D. J.: Linking the historic 2011 Mississippi River flood to coastal wetland sedimentation, Nat. Geosci., 5, 803–807, https://doi.org/10.1038/ngeo1615, 2012.

Fanelli, M., Illuminati, S., Annibaldi, A., De Marco, R., Cerotti, C., Girolametti, F., Ajdini, B., Truzzi, C., Frapiccini, E., Gallerani, A., Tramontana, M., Baldelli, G., and Spagnoli, F.: Mercury historical signature in the Central and Southern Adriatic Sea sediment cores, Estuar. Coast. Shelf Sci., 314, 109144, https://doi.org/10.1016/j.ecss.2025.109144, 2025.

Fazi, S., Baldassarre, L., Cassin, D., Quero, G. M., Pizzetti, I., Cibic, T., and Del Negro, P.: Prokaryotic community composition and distribution in coastal sediments following a Po river flood event (northern Adriatic Sea, Italy), Estuar. Coast. Shelf Sci., 233, 106547, https://doi.org/10.1016/j.ecss.2019.106547, 2020.

Field, J. A. and Seow, J.: Properties, occurrence, and fate of fluorotelomer sulfonates, Crit. Rev. Environ. Sci. Technol., 47, 643–691, https://doi.org/10.1080/10643389.2017.1326276, 2017.

Fowler, H. J., Lenderink, G., Prein, A. F., Westra, S., Allan, R. P., Ban, N., and Zhang, X.: Anthropogenic intensification of short-duration rainfall extremes, Nat. Rev. Earth Environ., 2, 107–122, https://doi.org/10.1038/s43017-020-00128-6, 2021.

Franzini, M., Leoni, L., and Saitta, M.: A simple method to evaluate the matrix effects in X-Ray fluorescence analysis, X-Ray Spectrom., 1, 151–154, https://doi.org/10.1002/xrs.1300010406, 1972.

Franzini, M., Leoni, L., and Saitta, M.: Revisione di una metodologia analitica per fluorescenza X, basata sulla correzione completa degli effetti di matrice, Rend. Soc. Ital. Mineral. Petrol., 31, 365–378, 1975.

Frapiccini, E., De Marco, R., Grilli, F., Marini, M., Annibaldi, A., Prezioso, E., Tramontana, M., and Spagnoli, F.: Anthropogenic contribution, transport, and accumulation of polycyclic aromatic hydrocarbons in sediments of the continental shelf and slope in the Mediterranean Sea, Chemosphere, 352, 141285, https://doi.org/10.1016/j.chemosphere.2024.141285, 2024.

Friedrichs, C. T. and Scully, M. E.: Modeling deposition by wave-supported gravity flows on the Po River prodelta: from seasonal floods to prograding clinoforms, Cont. Shelf Res., 27, 322–337, https://doi.org/10.1016/j.csr.2006.11.002, 2007.

Gao, C. and Guo, L.: Progress on microbial species diversity, community assembly and functional traits, Biodivers. Sci., 30, 168–180, 10.17520/biods.2022429, 2022.

Gao, X., Zhang, J., Yu, Z., Zhang, Y., and Chen, J.: Hydrological controls on nitrogen (ammonium versus nitrate) fluxes from river to coast in a subtropical region: Observation and modeling, J. Environ. Manage., 213, 382–391, https://doi.org/10.1016/j.jenvman.2018.02.071, 2018.

Gardner, J., Pavelsky, T., Topp, S., Yang, X., Ross, M. R., and Cohen, S.: Human activities change suspended sediment concentration along rivers, Environ. Res. Lett., 18, 064032, 10.1088/1748-9326/acd8d8, 2023.

Geyer, W. R., Hill, P., Milligan, T., and Traykovski, P.: The structure of the Eel River plume during floods, Cont. Shelf Res., 20, 2067–2093, https://doi.org/10.1016/S0278-4343(00)00063-5, 2000.

Gibson, R. N., Barnes, M., & Atkinson, R. J. A.: Impact of changes in flow of freshwater on estuarine and open coastal habitats and the associated organisms. Oceanography and marine biology: an annual review, 40, 233, 2002.

Giner-Lamia, J. and Huerta-Cepas, J.: Exploring the sediment-associated microbiota of the Mar Menor coastal lagoon, Front. Mar. Sci., 11, 1319961, https://doi.org/10.3389/fmars.2024.1319961, 2024.

Goodbred, S. L.: Response of the Ganges dispersal system to climate change: a source-to-sink view since the last interstade, Sediment. Geol., 162, 83–104, https://doi.org/10.1016/S0037-0738(03)00217-3, 2003.

Gomez, B., Mertes, L. A., Phillips, J. D., Magilligan, F. J., and James, L. A.: Sediment characteristics of an extreme flood: 1993 upper Mississippi River valley, Geology, 23, 963–966, https://doi.org/10.1130/0091-7613(1995)023<0963:SCOAEF>2.3.CO;2, 1995.

Govindaraju, K.: 1989 compilation of working values and sample description for 272 geostandards, Geostandards Newsletter, 13, 1–113, https://doi.org/10.1111/j.1751-908X.1989.tb00476.x, 1989.

Gruca-Rokosz, R., Cieśla, M., Kida, M., and Ignatowicz, K.: Spatio-Temporal Patterns of Polycyclic Aromatic Hydrocarbons and Phthalates Deposition in Sediments of Reservoirs: Impact of Some Environmental Factors, Water, 17, 641, 10.3390/w17050641, 2025.

Guild, R., Wang, X., and Quijón, P. A.: Climate change impacts on coastal ecosystems. Environmental Research: Climate, 3(4), 042006, 10.1088/2752-5295/ad9f90, 2024.

Gupta, D., Hazarika, B. B., Berlin, M., Sharma, U. M., and Mishra, K.: Artificial intelligence for suspended sediment load prediction: a review, Environ. Earth Sci., 80, 346, https://doi.org/10.1007/s12665-021-09625-3, 2021.

Hage, S., Galy, V. V., Cartigny, M. J. B., Acikalin, S., Clare, M. A., Gröcke, D. R., Jacinto, R. S., Vanneste, M., and Talling, P. J.: Efficient preservation of young terrestrial organic carbon in sandy turbidity-current deposits, Geology, 48, 882–887, https://doi.org/10.1130/G47212.1, 2020.

Hamamoto, K., Mizuyama, M., Nishijima, M., Maeda, A., Gibu, K., Poliseno, A., and Reimer, J. D.: Diversity, composition and potential roles of sedimentary microbial communities in different coastal substrates around subtropical Okinawa Island, Japan, Environ. Microbiome, 19, 54, https://doi.org/10.1186/s40793-024-00594-1, 2024.

Hanebuth, T. J., King, M. L., Lobo, F. J., & Mendes, I.: Formation history and material budget of holocene shelf mud depocenters in the Gulf of Cadiz. *Sedimentary Geology*, *421*, 105956, https://doi.org/10.1016/j.sedgeo.2021.105956, 2021.

Haq, B. and Milliman, J.: Perilous future for river deltas, GSA Today, 33, 4–12, 10.1130/GSATG566A.1, 2023.

Harris, C. K., Sherwood, C. R., Signell, R. P., Bever, A. J., and Warner, J. C.: Sediment dispersal in the northwestern Adriatic Sea, J. Geophys. Res.-Oceans, 113, C11, https://doi.org/10.1029/2006JC003868, 2008.

Hedges, J. I. and Keil, R. G.: Organic geochemical perspectives on estuarine processes: sorption reactions and consequences, Mar. Chem., 65, 55–65, https://doi.org/10.1016/S0304-4203(99)00012-X, 1999.

Hood, W. G.: Tidal channel meander formation by depositional rather than erosional processes: examples from the prograding Skagit River Delta (Washington, USA), Earth Surf. Process. Landforms, 35, 319–330, https://doi.org/10.1002/esp.1920, 2010.

Hort, H. M., Robinson, C. E., Sawyer, A. H., Li, Y., Cardoso, R., Lee, S. A., and Newell, C. J.: Conceptualizing controlling factors for PFAS salting out in groundwater discharge zones along sandy beaches, Groundwater, 62, 860–875, https://doi.org/10.1111/gwat.13428, 2024.

IPCC: Climate Change 2021: The Physical Science Basis. Contribution of Working Group I to the Sixth Assessment Report of the Intergovernmental Panel on Climate Change, Cambridge University Press, 2391 pp., https://doi.org/10.1017/9781009157896, 2021.

IPCC: Climate Change 2023: Synthesis Report. Contribution of Working Groups I, II and III to the Sixth Assessment Report of the Intergovernmental Panel on Climate Change [Core Writing Team, H. Lee and J. Romero (eds.)], IPCC, Geneva, Switzerland, 184 pp., 2023.

Jaramillo, S., Sheremet, A., Allison, M. A., Reed, A. H., and Holland, K. T.: Wave-mud interactions over the muddy Atchafalaya subaqueous clinoform, Louisiana, United States: Wave-supported sediment transport, J. Geophys. Res.-Oceans, 114, C4, https://doi.org/10.1029/2008JC004821, 2009.

Jeon, J., Kannan, K., Lim, B. J., An, K. G., and Kim, S. D.: Effects of salinity and organic matter on the partitioning of perfluoroalkyl acid (PFAs) to clay particles, J. Environ. Monit., 13, 1803–1810, https://doi.org/10.1039/C0EM00791A, 2011.

Jia, J., Bai, J., Gao, H., Wen, X., Zhang, G., Cui, B., and Liu, X.: In situ soil net nitrogen mineralization in coastal salt marshes (Suaeda salsa) with different flooding periods in a Chinese estuary, Ecol. Indic., 73, 559–565, https://doi.org/10.1016/j.ecolind.2016.10.038, 2017.

Jiajun, L., Biao, Z., Guangshuai, Z., Sihui, S., Yansong, L., Jinhui, Z., ... & Xiangyu, G.: Flooding promotes the coalescence of microbial community in estuarine habitats. *Marine Environmental Research*, *202*, 106735, https://doi.org/10.1016/j.marenvres.2024.106735, 2024.

Jolaosho, T. L., Rasaq, M. F., Omotoye, E. V., Araomo, O. V., Adekoya, O. S., Abolaji, O. Y., and Hungbo, J. J.: Microplastics in freshwater and marine ecosystems: Occurrence, characterization, sources, distribution dynamics, fate, transport processes, potential mitigation strategies, and policy interventions, Ecotoxicol. Environ. Saf., 294, 118036, 10.1016/j.ecoenv.2025.118036, 2025.

Korus, J. T. and Fielding, C. R.: Asymmetry in Holocene river deltas: patterns, controls, and stratigraphic effects, Earth-Sci. Rev., 150, 219–242, https://doi.org/10.1016/j.earscirev.2015.07.013, 2015.

Kuehl, S. A., Nittrouer, C. A., and DeMaster, D. J.: Distribution of sedimentary structures in the Amazon subaqueous delta. Continental Shelf Research, 6(1-2), 311-336, https://doi.org/10.1016/0278-4343(86)90066-X, 1986.

Kundzewicz, Z. W., Kanae, S., Seneviratne, S. I., Handmer, J., Nicholls, N., Peduzzi, P., and Sherstyukov, B.: Flood risk and climate change: global and regional perspectives, Hydrol. Sci. J., 59, 1–28, https://doi.org/10.1080/02626667.2013.857411, 2014.

Lazar, O. R., Bohacs, K. M., Schieber, J., Macquaker, J. H., and Demko, T. M.: Mudstone Primer: Lithofacies variations, diagnostic criteria, and sedimentologic–stratigraphic implications at lamina to bedset scale, SEPM Soc. Sediment. Geol., Tulsa, OK, USA, 192 pp., https://doi.org/10.2110/sepmcsp.12., 2015.

Lee, C. C., Chen, C. S., Wang, Z. X., and Tien, C. J.: Polycyclic aromatic hydrocarbons in 30 river ecosystems, Taiwan: sources, and ecological and human health risks, Sci. Total Environ., 795, 1–14, https://doi.org/10.1016/j.scitotenv.2021.148867, 2021.

Lehmann, J., Coumou, D., and Frieler, K.: Increased record-breaking precipitation events under global warming, Clim. Change, 132, 501–515, 2015. https://doi.org/10.1007/s10584-015-1434-y,

Leoni, L. and Saitta, M.: Determination of yttrium and niobium on standard silicate rocks by X-ray fluorescence analyses, X-Ray Spectrom., 5, 29–30, . https://doi.org/10.1002/xrs.1300050107, 1976

Leoni, L., Menichini, M., and Saitta, M.: Determination of S, Cl and F in silicate rocks by X-Ray fluorescence analyses, X-Ray Spectrom., 11, 156–158, https://doi.org/10.1002/xrs.1300110404, 1982.

Li, C., Zhang, C., Gibbes, B., Wang, T., and Lockington, D.: Coupling effects of tide and salting-out on perfluorooctane sulfonate (PFOS) transport and adsorption in a coastal aquifer, Adv. Water Resour., 166, 104240, https://doi.org/10.1016/j.advwatres.2022.104240, 2022.

Li, J., Zhang, B., Zhang, G., Shao, S., Li, Y., Zhang, J., Wang, J., and Guan, X.: Flooding promotes the coalescence of microbial community in estuarine habitats, Mar. Environ. Res., 202, 106735, https://doi.org/10.1016/j.marenvres.2024.106735, 2024.

Lim, K. Y., Zakaria, N. A., and Foo, K. Y.: Geochemistry pollution status and ecotoxicological risk assessment of heavy metals in the Pahang River sediment after the high magnitude of flood event, Hydrol. Res., 52, 107–124, https://doi.org/10.2166/nh.2020.122, 2021.

Lin, J., Zhang, J., Yu, Z., Gao, X., Chen, J., and Wei, Y.: Simultaneous observations revealed the non-steady state effects of a tropical storm on the export of particles and inorganic nitrogen through a river–estuary continuum, J. Hydrol., 606, 127438, https://doi.org/10.1016/j.jhydrol.2022.127438, 2022.

Lin, C., Bao, R., Zhu, L., Hu, R., Ji, J., and Yu, S.: Surface sediment erosion characteristics and influencing factors in the subaqueous delta of the abandoned Yellow River Estuary. Marine Geology, 468, 107219, https://doi.org/10.1016/j.margeo.2024.107219, 2024.

Liu, J. P., Li, A. C., Xu, K. H., Velozzi, D. M., Yang, Z. S., Milliman, J. D., and DeMaster, D. J.: Sedimentary features of the Yangtze River-derived along-shelf clinoform deposit in the East China Sea, Cont. Shelf Res., 26, 2141–2156, https://doi.org/10.1016/j.csr.2006.07.013, 2006.

Liu, J., Zhu, S., Liu, X., Yao, P., Ge, T., and Zhang, X.-H.: Spatiotemporal dynamics of the archaeal community in coastal sediments: assembly process and co-occurrence relationship, ISME J., 14, 1463–1478, https://doi.org/10.1038/s41396-020-0621-3, 2020.

Lohrenz, S. E., Dagg, M. J., and Whitledge, T. E.: Enhanced primary production at the plume/oceanic interface of the Mississippi River, Cont. Shelf Res., 10, 639–664, https://doi.org/10.1016/0278-4343(90)90043-L, 1990.

Lohmann, R., MacFarlane, J. K., and Gschwend, P. M.: Importance of black carbon to sorption of native PAHs, PCBs, and PCDDs in Boston and New York harbor sediments, Environ. Sci. Technol., 39, 141–148, https://doi.org/10.1021/es049424s, 2005.

Lucchini, F., Frignani, M., Sammartino, I., Dinelli, E., and Bellucci, L. G.: Composition of Venice Lagoon sediments: distribution, sources, settings and recent evolution, GeoActa, 1, 7–20, 2001.

Macquaker, J. H., Bentley, S. J., and Bohacs, K. M.: Wave-enhanced sediment-gravity flows and mud dispersal across continental shelves: Reappraising sediment transport processes operating in ancient mudstone successions, Geology, 38, 947–950, https://doi.org/10.1130/B30182.1, 2010.

Maletić, S. P., Beljin, J. M., Rončević, S. D., Grgić, M. G., and Dalmacija, B. D.: State of the art and future challenges for polycyclic aromatic hydrocarbons in sediments: sources, fate, bioavailability and remediation techniques, J. Hazard. Mater., 365, 467–482, https://doi.org/10.1016/j.jhazmat.2018.11.020, 2019.

Mali, M., Ragone, R., Dell'Anna, M. M., Romanazzi, G., Damiani, L., and Mastrorilli, P.: Improved identification of pollution source attribution by using PAH ratios combined with multivariate statistics, Sci. Rep., 12, 1–13, https://doi.org/10.1038/s41598-022-23966-4, 2022.

Mancuso, M., Bruno, C. A., Guardamagna, I., Mghili, B., Fabrizi, F., Nibali, V. C., and Bottari, T.: Anthropogenic particles accumulation in sea cucumbers: insights from a transitional environment. Marine Pollution Bulletin, 226, 119341, https://doi.org/10.1016/j.marpolbul.2026.119341, 2026.

Martin, M.: Cutadapt removes adapter sequences from high-throughput sequencing reads, EMBnet J., 17, 10–12, https://doi.org/10.14806/ej.17.1.200, 2011.

Massaccesi, N., Basili, M., Coci, M., Cassin, D., Zonta, R., Manini, E., and Quero, G. M.: Benthic prokaryotic diversity in Po River Delta lagoons (North Adriatic Sea) is shaped by riverine freshwater inputs, Estuar. Coast. Shelf Sci., 109348, https://doi.org/10.1016/j.ecss.2025.109348, 2025.

McMurdie, P. J. and Holmes, S.: phyloseq: an R package for reproducible interactive analysis and graphics of microbiome census data, PLoS ONE, 8, e61217, https://doi.org/10.1371/journal.pone.0061217, 2013.

Merz, B., Blöschl, G., Vorogushyn, S., Dottori, F., Aerts, J. C., Bates, P., and Macdonald, E.: Causes, impacts and patterns of disastrous river floods, Nat. Rev. Earth Environ., 2, 592–609, https://doi.org/10.1038/s43017-021-00195-3, 2021.

Milliman, J. D., and Meade, R. H.: World-wide delivery of river sediment to the oceans. The Journal of Geology, 91(1), 1-21, https://doi.org/10.1086/628741, 1983.

Milliman, J. D. and Syvitski, J. P.: Geomorphic/tectonic control of sediment discharge to the ocean: the importance of small mountainous rivers, J. Geol., 100, 525–544, https://doi.org/10.1086/629606, 1992.

MSFD: Directive 2008/56/EC of the European Parliament and of the Council establishing a framework for community action in the field of marine environmental policy (Marine Strategy Framework Directive), Off. J. Eur. Union, L 164, 19–40, 2008.

Munoz, G., Budzinski, H., and Labadie, P.: Influence of environmental factors on the fate of legacy and emerging per- and polyfluoroalkyl substances along the salinity/turbidity gradient of a macrotidal estuary, Environ. Sci. Technol., 51, 12347–12357, 10.1021/acs.est.7b03626, 2017.

Nascimento, R. A., de Almeida, M., Escobar, N. C., Ferreira, S. L., Mortatti, J., and Queiroz, A. F.: Sources and distribution of polycyclic aromatic hydrocarbons (PAHs) and organic matter in surface sediments of an estuary under petroleum activity influence, Todos os Santos Bay, Brazil, Mar. Pollut. Bull., 119, 223–230, https://doi.org/10.1016/j.marpolbul.2017.03.040, 2017.

Nakatsu, C. H., Byappanahalli, M. N., and Nevers, M. B.: Bacterial community 16S rRNA gene sequencing characterizes riverine microbial impact on Lake Michigan, Front. Microbiol., 10, 996, https://doi.org/10.3389/fmicb.2019.00996, 2019.

Neff, J. M., Stout, S. A., and Gunster, D. G.: Ecological risk assessment of polycyclic aromatic hydrocarbons in sediments: identifying sources and ecological hazard, Integr. Environ. Assess. Manag., 1, 22–23, https://doi.org/10.1897/IEAM_2004a-016.1, 2005.

Newell, C. J., Javed, H., Li, Y., Johnson, N. W., Richardson, S. D., Connor, J. A., and Adamson, D. T.: Enhanced attenuation (EA) to manage PFAS plumes in groundwater. Remediation Journal, 32(4), 239-257, https://doi.org/10.1002/rem.21731, 2022.

Nie, J., Sobel, A. H., Shaevitz, D. A., and Wang, S.: Dynamic amplification of extreme precipitation sensitivity, Proc. Natl. Acad. Sci. USA, 115, 9467–9472, https://doi.org/10.1073/pnas.1800357115, 2018.

Nikki, R., Jaleel, K. A., Razaque, M. A., Gupta, P., Rathore, C., Saha, M., and Kumar, T. G.: Assessment of hazardous microplastic polymers and phthalic acid esters in an invasive mollusk (Mytella strigata) from the Cochin estuary, southwest coast of India: Unraveling ecosystem risks, Sci. Total Environ., 967, 178798, https://doi.org/10.1016/j.scitotenv.2025.178798, 2025.

Ning, D., Wang, Y., Fan, Y., Wang, J., Van Nostrand, J. D., Wu, L., and Zhou, J.: Environmental stress mediates groundwater microbial community assembly. Nature Microbiology, 9(2), 490-501, https://doi.org/10.1038/s41564-023-01573-x, 2024.

Nittrouer, C. A., Kuehl, S. A., DeMaster, D. J., and Kowsmann, R. O.: The deltaic nature of Amazon shelf sedimentation, Geol. Soc. Am. Bull., 97, 444–458, https://doi.org/10.1130/0016-7606(1986)97<444:TDNOAS>2.0.CO;2, 1986.

Nogarotto, A., Noormets, R., Chauhan, T., Mollenhauer, G., Hefter, J., Grotheer, H., Weiner, S., Meyer, V. D., Pellegrini, C., and Tesi, T.: Coastal permafrost was massively eroded during the Bølling–Allerød warm period, Commun. Earth Environ., 4, 350, https://doi.org/10.1038/s43247-023-01046-5, 2023.

Ohenhen, L. O., Shirzaei, M., Davis, J. L., Tiwari, A., Nicholls, R., Dasho, O., and Yemele, G. C.: Global subsidence of river deltas, Nature, 1–8, https://doi.org/10.1038/s41586-026-XXXX-X, 2026.

Oksanen, J., Simpson, G. L., Blanchet, F. G., Kindt, R., Legendre, P., Minchin, P. R., O'Hara, R. B., Solymos, P., Stevens, M. H. H., Szoecs, E., and Wagner, H.: vegan: Community Ecology Package, R package version 2.6-8, CRAN [code], https://cran.r-project.org/package=vegan, 2025.

Overeem, I. and Brakenridge, R. G. (Eds.): Dynamics and vulnerability of delta systems, GKSS Research Centre, LOICZ Internat. Project Office, Inst. for Coastal Research, Vol. 35, 2009.

Owowenu, E. K., Nnadozie, C. F., Akamagwuna, F., Siwe-Noundou, X., and Odume, O. N.: Occurrence and distribution of microplastics in functionally delineated hydraulic zones in selected rivers, Eastern Cape, South Africa, Environ. Pollut., 126544, https://doi.org/10.1016/j.envpol.2025.126544, 2025.

Palinkas, C. M. and Nittrouer, C. A.: Clinoform sedimentation along the Apennine shelf, Adriatic Sea, Mar. Geol., 234, 245–260, https://doi.org/10.1016/j.margeo.2006.09.006, 2006.

Palinkas, C. M. and Nittrouer, C. A.: Modern sediment accumulation on the Po shelf, Adriatic Sea, Cont. Shelf Res., 27, 489–505, https://doi.org/10.1016/j.csr.2006.11.006, 2007.

Parada, A. E., Needham, D. M., and Fuhrman, J. A.: Every base matters: assessing small subunit rRNA primers for marine microbiomes with mock communities, time series and global field samples, Environ. Microbiol., 18, 1403–1414, https://doi.org/10.1111/1462-2920.13023, 2016.

Peng, Y., Yu, Q., Du, Z., Wang, L., Wang, Y., and Gao, S.: Gravity-driven sediment flows on the shallow sea floor of a muddy open coast, Mar. Geol., 445, 106759, https://doi.org/10.1016/j.margeo.2022.106759, 2022.

Pellegrini, C., Maselli, V., Cattaneo, A., Piva, A., Ceregato, A., and Trincardi, F.: Anatomy of a compound delta from the post-glacial transgressive record in the Adriatic Sea, Mar. Geol., 362, 43–59, https://doi.org/10.1016/j.margeo.2015.01.010, 2015.

Pellegrini, C., Patruno, S., Helland-Hansen, W., Steel, R. J., and Trincardi, F.: Clinoforms and clinothems: Fundamental elements of basin infill, Basin Res., 32, 187–205, https://doi.org/10.1111/bre.12446, 2020.

Pellegrini, C., Tesi, T., Schieber, J., Bohacs, K. M., Rovere, M., Asioli, A., and Trincardi, F.: Fate of terrigenous organic carbon in muddy clinothems on continental shelves revealed by stratal geometries: Insight from the Adriatic sedimentary archive, Global Planet. Change, 203, 103539, https://doi.org/10.1016/j.gloplacha.2021.103539, 2021.

Pellegrini, C., Saliu, F., Bosman, A., Sammartino, I., Raguso, C., Mercorella, A., and Rovere, M.: Hotspots of microplastic accumulation at the land-sea transition and their spatial heterogeneity: The Po River prodelta (Adriatic Sea), Sci. Total Environ., 895, 164908, https://doi.org/10.1016/j.scitotenv.2023.164908, 2023.

Pellegrini, C., Sammartino, I., Schieber, J., Tesi, T., Paladini de Mendoza, F., Rossi, V., and Amorosi, A.: On depositional processes governing along-strike facies variations of fine-grained deposits: Unlocking the Little Ice Age subaqueous clinothems on the Adriatic shelf, Sedimentology, 71, 941–973, https://doi.org/10.1111/sed.13162, 2024.

Pierdomenico, M., Ridente, D., Casalbore, D., Di Bella, L., Milli, S., and Chiocci, F. L.: Plastic burial by flash-flood deposits in a prodelta environment (Gulf of Patti, Southern Tyrrhenian Sea), Mar. Pollut. Bull., 181, 113819, https://doi.org/10.1016/j.marpolbul.2022.113819, 2022.

Pitarch, J., Falcini, F., Nardin, W., Brando, V. E., Di Cicco, A., and Marullo, S.: Linking flow-stream variability to grain size distribution of suspended sediment from a satellite-based analysis of the Tiber River plume (Tyrrhenian Sea), Sci. Rep., 9, 19729, https://doi.org/10.1038/s41598-019-56409-8, 2019.

Pizzini, S., Morabito, E., Gregoris, E., Vecchiato, M., Corami, F., Piazza, R., and Gambaro, A.: Occurrence and source apportionment of organic pollutants in deep sediment cores of the Venice Lagoon, Mar. Pollut. Bull., 164, 112053, https://doi.org/10.1016/j.marpolbul.2021.112053, 2021.

Pizzini, S., Giubilato, E., Morabito, E., Barbaro, E., Bonetto, A., Calgaro, L., and Marcomini, A.: Contaminants of emerging concern in water and sediment of the Venice Lagoon, Italy, Environ. Res., 249, 118401, https://doi.org/10.1016/j.envres.2024.118401, 2024.

Puig, P., Ogston, A. S., Guillén, J., Fain, A. M. V., and Palanques, A.: Sediment transport processes from the topset to the foreset of a crenulated clinoform (Adriatic Sea), Cont. Shelf Res., 27, 452–474, https://doi.org/10.1016/j.csr.2006.11.005, 2007.

Pulvirenti, L., Squicciarino, G., Fiori, E., Candela, L., and Puca, S.: Analysis and processing of the COSMO-SkyMed second generation images of the 2022 Marche (Central Italy) flood, Water, 15, 1353, https://doi.org/10.3390/w15071353, 2023.

Quero, G. M., Cassin, D., Botter, M., Perini, L., and Luna, G. M.: Patterns of benthic bacterial diversity in coastal areas contaminated by heavy metals, polycyclic aromatic hydrocarbons (PAHs) and polychlorinated biphenyls (PCBs), Front. Microbiol., 6, 1053, https://doi.org/10.3389/fmicb.2015.01053, 2015.

Reed, H. E. and Martiny, J. B. H.: Microbial composition affects the functioning of estuarine sediments, ISME J., 7, 868–879, https://doi.org/10.1038/ismej.2012.154, 2013.

Regione Marche: Studio sulle analisi ambientali in aria (aggiornato a giugno 2019), Dipartimento di Ingegneria Industriale e Scienze Matematiche, Università Politecnica delle Marche, last access: 20 June 2024, 2016.

Riminucci, F., Funari, V., Ravaioli, M., and Capotondi, L.: Trace metals accumulation on modern sediments from Po river prodelta, North Adriatic Sea, Mar. Pollut. Bull., 175, 113399, https://doi.org/10.1016/j.marpolbul.2022.113399, 2022.

Roberts, D. A.: Causes and ecological effects of resuspended contaminated sediments (RCS) in marine environments, Environ. Int., 40, 230–243, https://doi.org/10.1016/j.envint.2011.11.013, 2012.

Rockne, K. J., Shor, L. M., Young, L. Y., Taghon, G. L., and Kosson, D. S.: Distributed sequestration and release of PAHs in weathered sediment: the role of sediment structure and organic carbon properties, Environ. Sci. Technol., 36, 2636–2644, https://doi.org/10.1021/es015714u, 2002.

Roussiez, V., Ludwig, W., Monaco, A., Probst, J. L., Bouloubassi, I., Buscail, R., and Saragoni, G.: Sources and sinks of sediment-bound contaminants in the Gulf of Lions (NW Mediterranean Sea): a multi-tracer approach, Cont. Shelf Res., 26, 1843–1857, https://doi.org/10.1016/j.csr.2006.04.010, 2006.

Rozemeijer, J., Noordhuis, R., Ouwerkerk, K., Pires, M. D., Blauw, A., Hooijboer, A., and van Oldenborgh, G. J.: Climate variability effects on eutrophication of groundwater, lakes, rivers, and coastal waters in the Netherlands, Sci. Total Environ., 771, 145366, https://doi.org/10.1016/j.scitotenv.2021.145366, 2021.

Saliu, F., Lasagni, M., Andò, S., Ferrero, L., Pellegrini, C., Calafat, A., and Sanchez-Vidal, A.: A baseline assessment of the relationship between microplastics and plasticizers in sediment samples collected from the Barcelona continental shelf. Environmental Science and Pollution Research, 30(13), 36311-36324, https://doi.org/10.1007/s11356-022-24772-1, 2023.

Sammartino, I.: Heavy-metal anomalies and bioavailability from soils of southeastern Po Plain, GeoActa, 3, 35–42, 2004.

Schieber, J.: SEM observations on ion-milled samples of Devonian black shales from Indiana and New York: the petrographic context of multiple pore types, https://doi.org/10.1306/13391711M1023589, 2013.

Schimmelmann, A., Riese, D. J., and Schieber, J.: Fast and economical sampling and resin-embedding technique for small cores of unconsolidated, fine-grained sediment, in: Proceedings of the 2015 Pacific Climate (PACLIM) Workshop, Asilomar Conference Grounds, Pacific Grove, CA, USA, 8–11, 2015.

Semenza, J. C.: Cascading risks of waterborne diseases from climate change, Nat. Immunol., 21, 484–487, https://doi.org/10.1038/s41590-020-0648-8, 2020.

Sherwood, C. R., Book, J. W., and Harris, C. K.: Sediment dynamics in the Adriatic Sea investigated with coupled models, Oceanography, 17, 58, https://doi.org/10.5670/oceanog.2004.04, 2015.

Signell, R. P., Chiggiato, J., Horstmann, J., Doyle, J. D., Pullen, J., and Askari, F.: High-resolution mapping of Bora winds in the northern Adriatic Sea using synthetic aperture radar, J. Geophys. Res.-Oceans, 115, C4, https://doi.org/10.1029/2009JC005524, 2010.

Simon-Sánchez, L., Grelaud, M., Garcia-Orellana, J., and Ziveri, P.: River Deltas as hotspots of microplastic accumulation: The case study of the Ebro River (NW Mediterranean), Sci. Total Environ., 687, 1186–1196, https://doi.org/10.1016/j.scitotenv.2019.06.168, 2019.

Slater, L., Villarini, G., Archfield, S., Faulkner, D., Lamb, R., Khouakhi, A., and Yin, J.: Global changes in 20-year, 50-year, and 100-year river floods, Geophys. Res. Lett., 48, e2020GL091824, https://doi.org/10.1029/2020GL091824, 2021.

Soclo, H. H., Garrigues, P. H., and Ewald, M.: Origin of polycyclic aromatic hydrocarbons (PAHs) in coastal marine sediments: case studies in Cotonou (Benin) and Aquitaine (France) areas, Mar. Pollut. Bull., 40, 387–396, https://doi.org/10.1016/S0025-326X(99)00200-3, 2000.

Sommerfield, C. K. and Nittrouer, C. A.: Modern accumulation rates and a sediment budget for the Eel shelf: a flood-dominated depositional environment, Mar. Geol., 154, 227–241, https://doi.org/10.1016/S0025-3227(98)00105-8, 1999.

Steichen, J. L., Labonté, J. M., Windham, R., Hala, D., Kaiser, K., Setta, S., and others: Microbial, physical, and chemical changes in Galveston Bay following an extreme flooding event, Hurricane Harvey, Front. Mar. Sci., 7, 186, https://doi.org/10.3389/fmars.2020.00186, 2020.

Stout, S. A. and Emsbo-Mattingly, S. D.: Concentration and character of PAHs and other hydrocarbons in coals of varying rank – implications for environmental studies of soils and sediments containing particulate coal, Org. Geochem., 39, 801–819, https://doi.org/10.1016/j.orggeochem.2008.05.004, 2008.

Sun, Q., Zhang, X., Zwiers, F., Westra, S., and Alexander, L. V.: A global, continental, and regional analysis of changes in extreme precipitation, J. Clim., 34, 243–258, https://doi.org/10.1175/JCLI-D-19-0892.1, 2021.

Syvitski, J., Ángel, J. R., Saito, Y., Overeem, I., Vörösmarty, C. J., Wang, H., and Olago, D.: Earth's sediment cycle during the Anthropocene, Nat. Rev. Earth Environ., 3, 179–196, https://doi.org/10.1038/s43017-021-00253-w, 2022.

Syvitski, J. P. and Kettner, A. J.: On the flux of water and sediment into the Northern Adriatic Sea, Cont. Shelf Res., 27, 296–308, https://doi.org/10.1016/j.csr.2005.08.029, 2007.

Syvitski, J. P., Peckham, S. D., Hilberman, R., and Mulder, T.: Predicting the terrestrial flux of sediment to the global ocean: a planetary perspective, Sediment. Geol., 162, 5–24, https://doi.org/10.1016/S0037-0738(03)00232-X, 2003.

Syvitski, J. P., Vörösmarty, C. J., Kettner, A. J., and Green, P.: Impact of humans on the flux of terrestrial sediment to the global coastal ocean, Science, 308, 376–380, DOI: 10.1126/science.1109454, 2005.

Syvitski, J. P., Kettner, A. J., Overeem, I., Hutton, E. W., Hannon, M. T., Brakenridge, G. R., and Nicholls, R. J.: Sinking deltas due to human activities, Nat. Geosci., 2, 681–686, https://doi.org/10.1038/ngeo629, 2009.

Talley, J. W., Ghosh, U., Tucker, S. G., Furey, J. S., and Luthy, R. G.: Particle-scale understanding of the bioavailability of PAHs in sediment, Environ. Sci. Technol., 36, 477–483, https://doi.org/10.1021/es0106442, 2002.

Tesi, T., Miserocchi, S., Goñi, M. E. A., Langone, L., Boldrin, A., and Turchetto, M.: Organic matter origin and distribution in suspended particulate materials and surficial sediments from the western Adriatic Sea (Italy), Estuar. Coast. Shelf Sci., 73, 431–446, https://doi.org/10.1016/j.ecss.2007.02.008, 2007.

Tesi, T., Langone, L., Giani, M., Ravaioli, M., and Miserocchi, S.: Source, diagenesis, and fluxes of particulate organic carbon along the western Adriatic Sea (Mediterranean Sea), Mar. Geol., 337, 156–170, https://doi.org/10.1016/j.margeo.2013.03.001, 2013.

Traykovski, P., Wiberg, P. L., and Geyer, W. R.: Observations and modeling of wave-supported sediment gravity flows on the Po prodelta and comparison to prior observations from the Eel shelf, Cont. Shelf Res., 27, 375–399, https://doi.org/10.1016/j.csr.2005.07.008, 2007.

Trincardi, F., Amorosi, A., Bosman, A., Correggiari, A., Madricardo, F., and Pellegrini, C.: Ephemeral rollover points and clinothem evolution in the modern Po Delta based on repeated bathymetric surveys, Basin Res., 32, 402–418, https://doi.org/10.1111/bre.12426, 2020.

Trincardi, F., Francocci, F., Pellegrini, C., d'Alcalà, M. R., and Sprovieri, M.: The Mediterranean Sea in the Anthropocene, in: Oceanography of the Mediterranean Sea, Elsevier, 501–553, https://doi.org/10.1016/B978-0-12-823692-5.00013-3, 2023.

Trouche, B., Brandt, M. I., Belser, C., Orejas, C., Pesant, S., Poulain, J., Wincker, P., Auguet, J.-C., Arnaud-Haond, S., and Maignien, L.: Diversity and biogeography of bathyal and abyssal seafloor bacteria and archaea along a Mediterranean–Atlantic gradient, Front. Microbiol., 12, 702016, https://doi.org/10.3389/fmicb.2021.702016, 2021.

Ukalska-Jaruga, A., Smreczak, B., and Klimkowicz-Pawlas, A.: Soil organic matter composition as a factor affecting the accumulation of polycyclic aromatic hydrocarbons, J. Soils Sediments, 19, 1890–1900, https://doi.org/10.1007/s11368-018-02225-1, 2019.

Vane, C. H., Harrison, I., and Kim, A. W.: Polycyclic aromatic hydrocarbons (PAHs) and polychlorinated biphenyls (PCBs) in sediments from the Mersey Estuary, UK, Sci. Total Environ., 374, 112–126, https://doi.org/10.1016/j.scitotenv.2006.12.012, 2007.

Vane, C. H., Kim, A. W., Emmings, J. F., Turner, G. H., Moss-Hayes, V., Lort, J. A., and Williams, P. J.: Grain size and organic carbon controls polyaromatic hydrocarbons (PAH), mercury (Hg) and toxicity of surface sediments in the River Conwy Estuary, Wales, UK, Mar. Pollut. Bull., 158, 111412, https://doi.org/10.1016/j.marpolbul.2020.111412, 2020.

Vörösmarty, C. J., Meybeck, M., Fekete, B., Sharma, K., Green, P., and Syvitski, J. P.: Anthropogenic sediment retention: major global impact from registered river impoundments, Global Planet. Change, 39, 169–190, https://doi.org/10.1016/S0921-8181(03)00023-7, 2003.

Voynova, Y. G., Petersen, W., Gehrung, M., Bremm, C., Winde, V., Böttcher, M. E., and Emeis, K.-C.: Extreme flood impact on estuarine and coastal biogeochemistry: the 2013 Elbe flood, Biogeosciences, 14, 541–557, https://doi.org/10.5194/bg-14-541-2017, 2017.

Wang, S., Wang, H., and Deng, W.: Perfluorooctane sulfonate (PFOS) distribution and effect factors in the water and sediment of the Yellow River Estuary, China, Environ. Monit. Assess., 185, 8517–8524, https://doi.org/10.1007/s10661-013-3192-5, 2013.

Wang, Y., Hong, Y., Ma, M., Wu, S., Op den Camp, H. J., Zhu, G., and Ye, F.: Anthropogenic pollution intervenes the recovery processes of soil archaeal community composition and diversity from flooding. *Frontiers in Microbiology*, *10*, 2285, https://doi.org/10.3389/fmicb.2019.02285, 2019.

Wang, X. H. and Pinardi, N.: Modeling the dynamics of sediment transport and resuspension in the northern Adriatic Sea, J. Geophys. Res.-Oceans, 107, C12, 18-1, https://doi.org/10.1029/2001JC001303, 2002.

Warrick, J. A., Buscombe, D., Vos, K., Bryan, K. R., Castelle, B., Cooper, J. A. G., and Young, A. P.: Coastal shoreline change assessments at global scales, Nat. Commun., 15, 2316, https://doi.org/10.1038/s41467-024-46608-x, 2024.

Weiss, L., Estournel, C., Marsaleix, P., Mikolajczak, G., Constant, M., and Ludwig, W.: From source to sink: part 1—characterization and Lagrangian tracking of riverine microplastics in the Mediterranean Basin, Environ. Sci. Pollut. Res., 1–24, https://doi.org/10.1007/s11356-024-34635-6, 2025.

Wentworth, C. K.: A scale of grade and class terms for clastic sediments, J. Geol., 30, 377–392, https://doi.org/10.1086/622910, 1922.

Westra, S., Alexander, L. V., and Zwiers, F. W.: Global increasing trends in annual maximum daily precipitation, J. Clim., 26, 3904–3918, https://doi.org/10.1175/JCLI-D-12-00502.1, 2013.

Wheatcroft, R. A.: Oceanic flood sedimentation: a new perspective, Cont. Shelf Res., 20, 2059–2066, https://doi.org/10.1016/S0278-4343(00)00062-5, 2000.

Wheatcroft, R. A. and Drake, D. E.: Post-depositional alteration and preservation of sedimentary event layers on continental margins, I. The role of episodic sedimentation, Mar. Geol., 199, 123–137, https://doi.org/10.1016/S0025-3227(03)00146-4, 2003.

Wheatcroft, R. A.: Time-series measurements of macrobenthos abundance and sediment bioturbation intensity on a flood-dominated shelf, Prog. Oceanogr., 71, 88–122, https://doi.org/10.1016/j.pocean.2006.07.001, 2006.

Winsemius, H. C., Aerts, J. C., Van Beek, L. P., Bierkens, M. F., Bouwman, A., Jongman, B., and Ward, P. J.: Global drivers of future river flood risk, Nat. Clim. Chang., 6, 381–385, https://doi.org/10.1038/nclimate2893, 2016.

Xin, Y., Zhang, J., Lu, T., Wei, Y., and Shen, P.: Response of prokaryotic, eukaryotic and algal communities to heavy rainfall in a reservoir supplied with reclaimed water, J. Environ. Manage., 334, 117394, https://doi.org/10.1016/j.jenvman.2023.117394, 2023.

Yao, J., Zhang, J., Lin, J., Yu, Z., Gao, X., Wei, Y., and Chen, J.: Hydro-climatological drivers of the unprecedented flooding in August 2022 along the Tarim River, China, J. Hydrol., 639, 131630, https://doi.org/10.1016/j.jhydrol.2024.131630, 2024.

Yin, C., Pan, C. G., Xiao, S. K., Wu, Q., Tan, H. M., and Yu, K.: Insights into the effects of salinity on the sorption and desorption of legacy and emerging per- and polyfluoroalkyl substances (PFASs) on marine sediments, Environ. Pollut., 300, 118957, https://doi.org/10.1016/j.envpol.2022.118957, 2022.

Yunker, M. B., Macdonald, R. W., Vingarzan, R., Mitchell, R. H., Goyette, D., and Sylvestre, S.: PAHs in the Fraser River basin: a critical appraisal of PAH ratios as indicators of PAH source and composition, Org. Geochem., 33, 489–515, https://doi.org/10.1016/S0146-6380(02)00002-5, 2002.

Zhang, M., Krom, M. D., Lin, J., Cheng, P., and Chen, N.: Effects of a storm on the transformation and export of phosphorus through a subtropical river–turbid estuary continuum revealed by continuous observation, J. Geophys. Res.-Biogeosci., 127, e2022JG006786, https://doi.org/10.1029/2022JG006786, 2022.

Zhang, L., Li, Y., Sun, X., Adams, J. M., Wang, L., Zhang, H., and Chu, H.: More robust co-occurrence patterns and stronger dispersal limitations of bacterial communities in wet than dry seasons of riparian wetlands, mSystems, 8, e01187-22, https://doi.org/10.1128/msystems.01187-22, 2023.